

**AEROSOL RADIATIVE FORCING DURING THE PRE-MONSOON TO  
MONSOON TRANSITION OVER THE INDIAN MONSOON REGION**

*by*

**ANAGHA P S**

**(2016 - 20 - 016)**

**THESIS**

**Submitted in partial fulfillment of the requirement for the degree of**

**BSc-MSc (Integrated) Climate Change Adaptation**

**Faculty of Agriculture**

**Kerala Agricultural University**



**COLLEGE OF CLIMATE CHANGE AND ENVIRONMENTAL  
SCIENCE**

**VELLANIKKARA, THRISSUR – 680656**

**KERALA, INDIA**

**2021**

## DECLARATION

I, Anagha, P. S. hereby declare that this thesis entitled “**Aerosol radiative forcing during the pre-monsoon to monsoon transition over the Indian monsoon region**” is a bona fide record of research work done by me during the course of research and the thesis has not been previously formed the basis for the award of any degree, diploma, associateship, fellowship or other similar title, of any other University or Society.

Place: Vellanikkara

Anagha P S

Date:

2016 - 20 - 2016

## **CERTIFICATE**

I, hereby certify that the thesis entitled “**Aerosol radiative forcing during the pre-monsoon to monsoon transition over the Indian monsoon region**” is a record of research work done independently by Ms. Anagha P S (2016 - 20 - 016) under my guidance and supervision and that it has not previously formed the basis for the award of any degree, diploma, fellowship or associateship to her.

Place: Kochi

Date:

**Dr. M. G. Manoj**

Major advisor, advisory committee

Scientist - D

Advanced Centre for Atmospheric  
Radar Research (ACARR)

Cochin University of Science and  
Technology (CUSAT)

Kalamassery, Kochi – 682022, Kerala



## ACKNOWLEDGEMENT

*The success and final outcome of this thesis work required a great deal of guidance and assistance from many people, all of whom deserve my deepest gratitude, and I consider myself extremely fortunate to have received this throughout the completion of my thesis work.*

*I would like to express my heartfelt respect and sincere gratitude to my major advisor **Dr. M. G Manoj**; Scientist -D & Academic Co-ordinator, Advanced Centre for Atmospheric Radar Research (ACARR), Cochin University of Science and Technology, Kalamassery, for the useful comments, remarks, guidance and support throughout the learning process of this master's thesis. His advice was extremely beneficial throughout the research and writing of this thesis.*

*I would like to express my heartfelt gratitude to our beloved dean, Prof. **P. O. Nameer** (PhD), College of Climate Change and Environmental Science (CCCES), Kerala Agriculture University (KAU), Vellanikkara, and member of my advisory committee, for his unwavering support, motivation, expert advice, and sharing immense continuous support of my entire course study and related research.*

*I would also like to thank **Dr. S. Abhilash**, Associate Director, ACARR, CUSAT, Kalamassery, and **Dr. P. Vijay Kumar**, Scientist, ACARR, CUSAT, Kalamassery, for providing me with the resources I needed to finish my work.*

*I would like to give special thanks to **all ACAR faculty and project students** for their unswerving assistance and motivation throughout my thesis work.*

*I'd like to express my profound gratitude to **Mrs. Krishnapriya** and **Dr. Jayakrishnan P.R** for their insightful suggestions and assistance.*

*I gratefully acknowledge **Dr. Gopakumar C.S.**, Scientific Officer, CCCES, KAU, for his valuable blessings and comments on my research. I was always inspired by the useful conversations I had with him, both inside and outside of college.*

*I sincerely thank each and **every member** of my CCCES for their aid and encouragement. My heartfelt thank and love to my **batchmates** of Campeones - 2016 for their valuable comments and suggestions on my paper, which inspired me to improve the quality of my work. My heartfelt gratitude goes to all of my **senior batches** for their help and support and valuable suggestions.*

*Last but not least, I would like to dedicate this thesis to **my parents** for their unwavering support, love, and encouragement in keeping my passion alive and spiritually supporting me while writing this thesis and my life in general.*

*Above all, I bow my head in gratitude to the Almighty for the blessings bestowed upon me in successfully completing the thesis.*

**Anagha P S**

## TABLE OF CONTENTS

---

<b>CHAPTER NO:</b>	<b>NAME OF THE CHAPTER</b>	<b>PAGE NO:</b>
	<b>LIST OF TABLES</b>	<b>i</b>
	<b>LIST OF FIGURES</b>	<b>ii - iv</b>
	<b>SYMBOLS AND ABBREVIATIONS</b>	<b>v - vii</b>
<b>1</b>	<b>INTRODUCTION</b>	<b>1 - 3</b>
<b>2</b>	<b>REVIEW OF LITERATURE</b>	<b>4 - 29</b>
<b>3</b>	<b>MATERIALS AND METHODS</b>	<b>30 - 43</b>
<b>4</b>	<b>RESULTS</b>	<b>44 - 62</b>
<b>5</b>	<b>DISCUSSION</b>	<b>63 - 65</b>
<b>6</b>	<b>SUMMARY AND CONCLUSION</b>	<b>66-67</b>
<b>7</b>	<b>REFERENCES</b>	<b>68-77</b>
	<b>ABSTRACT</b>	

## LIST OF TABLES

<b>TABLE NO:</b>	<b>TITLE</b>	<b>PAGE NO:</b>
1	Satellite derived daily and monthly data used in this study	38
2	Categorization of transition period into sub-periods	49
3	Classification of aerosol types based on AOD	45
4	Values for aerosol radiative forcing at the top of the atmosphere, surface and atmosphere during transition phase, advancing phase and peak phases of monsoon	55



## LIST OF FIGURES

FIGURE NO:	TITLE	PAGE NO:
1	Schematic depiction of the direct radiative effect of aerosols. Adapted from “Climate effects of dust aerosols over East Asian arid and semiarid regions” by, Huang et al., 2014	15
2	Schematic depiction of the indirect radiative effect of aerosols. Adapted from “Climate effects of dust aerosols over East Asian arid and semiarid regions” by, Huang et al., 2014	16
3	Schematic depiction of the semi-direct radiative effect of aerosols. Adapted from “Climate effects of dust aerosols over East Asian arid and semiarid regions” by, Huang et al., 2014	18
4	Schematic representation of monsoon water cycle during normal and EHP induced condition. Adapted from “The Joint Aerosol–Monsoon Experiment: A New Challenge for Monsoon Climate Research” by, Lau et al., 2008	27
5	Schematic representation of spatial coverage of study area comprising 5 <sup>0</sup> S, 50 <sup>0</sup> E to 40 <sup>0</sup> N, 110 <sup>0</sup> E	31
6	Temporal average of AOD over Indian monsoon region during the period of study	43

7	Temporal average of AOD during the south west monsoon over the Indian monsoon region during the period of study	45
8	Intraseasonal variation of spatial distribution of aerosols during summer monsoon from 2017 to 2020. (a) Composite average of AOD during the transition phase, (b) Composite average of AOD during the advancing phase, and (c) Composite average of AOD during the peak phase.	47
9	Mean of surface westerlies (m/s) at 850hPa during the subperiods of transition phase from 2017-2020 using ERA5 reanalysis	49
10	Aerosol species wise contribution over the Indian monsoon region over the period of study	51
11	Composite Aerosol Index during a) transition period, b)advancing period, c) peak period and the d) wet monsoon period over Indian monsoon region for a period of 2017-2020	52
12	composite average of intraseasonal aerosol radiative forcing over a period of 2017-2020 during, a) transition period, b) advancing period and c) peak period over a period of 2017-2020	54
13	Graphical representation of aerosol induced atmospheric radiative forcing over Indo Gangetic Plain and Equatorial Indian Ocean during a) transition phase, b) advancing phase, and c) peak phase.	57

14	Vertical profile for aerosol induced heating rate over the Indo Gangetic Plain during pre-monsoon, monsoon and post-monsoon	58-59
15	Aerosol-rainfall association over Kerala and Indo Gangetic Plain over a period of 2017-2020	61-62

## SYMBOLS AND ABBREVIATIONS

%	Percentage
$\partial T/\partial T$	Aerosol Heating Rate
ADAS	Atmospheric Data Assimilation System
AI	Aerosol Index
AIvE	Aerosol-Induced Cloud Invigoration Effect
AOD	Aerosol Optical Depth
AOT	Aerosol Optical Thickness
$ARF_{(ATM)}$	Aerosol Radiative Forcing In The Atmosphere
$ARF_{(SRF)}$	Aerosol Radiative Forcing at the Surface
$ARF_{(TOA)}$	Aerosol Radiative Forcing at the Top Of Atmosphere
B	Aerosol Load
BC	Black Carbon
CAM	Community Atmosphere Model
CCN	Cloud Condensation Nuclei
CERES	Clouds and the Earth's Radiant Energy System
CP	Specific Heat At Constant Pressure
D	Path Length
DB	Deep Blue
DRF	Direct Radiative Effect
DT	Dark Target
ECMRWF	European Centre for Medium-Range Weather Forecasts
EHP	Elevated Heat Pump
EIO	Equatorial Indian Ocean
ENSO	El-Nino Southern Oscillation
EOS	Earth Observing System
ERB	Earth Radiation Budget
$F_{(all\ sky)}$	Net Flux with All Sky Condition
$F_{(noaero)}$	Net Flux with All Sky No Aerosol Condition
FM	Flight Models

G	Gravitational Acceleration
GEOS-5	Goddard Earth Observing System Model, Version 5
GPC	Gas to Particle Conversion
hPa	Hectopascal
$I_{\text{calc}}$	Estimated Radiance
IGB	Indo Gangetic Plain
$I_{\text{meas}}$	Measured Backscatter Radiance
ITCZ	Inter-Tropical Convergence Zone
$L_{\text{(down)}}$	Back scattered long wave radiation
$L_{\text{(up)}}$	Up scattered long wave radiation
MARC	Model For Research Of Climate
mbar	Millibar
MERRA-2	Modern-Era Retrospective Analysis for Research and Applications, Version 2
MISR	Multi-Angle Imaging Spectroradiometer
MODIS	Moderate Resolution Imaging Spectroradiometer
nm	Nanometre
NOAA	National Oceanic and Atmosphere Administration
NPP	National Polar-Orbiting Partnership
OC	Organic Carbon
OMI	Ozone Monitoring Instrument
R	Removal Flux
$R_{\text{net}}$	Net flux
S	Source Flux
$S_{\text{(down)}}$	Surface reaching short wave radiation
$S_{\text{(up)}}$	Up scattered short wave radiation
SBDART	Santa Barbara Discrete Ordinate Radiative Transfer
SRF	Surface Radiative Flux
SSA	Single Scattering Albedo
SST	Sea Surface Temperature
t	Residence Time
T	Transmissivity
TOA	Top Of Atmosphere

TOMS	Total Ozone Mapping Spectrometer
TP	Tibetan Plateau
UV	Ultra Violet
W/m <sup>2</sup>	Watts/metre <sup>2</sup>
B	Absorption Coefficient
ΔP	Vertical Extend Of Atmosphere
T	Aerosol Optical Depth

## CHAPTER 1

### INTRODUCTION

The precise prediction of the Indian summer monsoon rainfall and circulation is critical for India and certainly relevant for other regions of the world, as anomalies in the monsoon often have severe economic and societal effects in a global scale. The Indian subcontinent receives approximately 80% of its rainfall during the southwest monsoon season. As the southwest trade winds strengthen, the branch of the inter-tropical convergence zone (ITCZ), a low-pressure belt that propagates pole ward more prominently over the Indian subcontinent, is known simultaneously as the monsoon trough, and transports large amounts of moisture from the ocean to the Indian subcontinent. In a densely populated and environmentally sensitive region like India, understanding ISM variability associated with synoptic weather systems such as monsoon depressions, low-pressure systems, and extra-tropical disturbances on different time scales is critical for successful risk management and adaptation planning. The predictability of the Indian monsoon may be influenced by the relative contributions of internal monsoon dynamics and external forcings such as sea surface temperature (SST), Tibetan Plateau heating that act as heat source during summer monsoon, soil moisture, Eurasian snow cover, greenhouse gas concentration, aerosol induced radiative forcings, teleconnection patterns (large scale atmospheric variability patterns) known to influence the variability of Indian monsoon rainfall (Sajani *et al.*, 2012), in which aerosol playing a particularly important role in controlling large-scale circulations by reducing or enhancing the land–ocean thermal contrast and inter-hemispheric energy imbalance. Thus, aerosols can be considered as globally recognized climate forcing agents contributing to regional and global climate change. Aerosol-monsoon interactions, and their incorporation into modeling studies, are found to be significant factors not only for analyzing climate change, but also for short-term weather forecasts and, more likely, medium to long-term forecasts and seasonal-to-interannual Asian monsoon predictions (Lau *et al.*, 2017). Aerosols

have a complex nature due to their heterogeneity in size, chemical properties, optical properties, concentration, ambient conditions, and so on. In addition, seasonal sources of aerosols during the summer monsoon also contribute to the complexity of aerosols in controlling radiation budgets (Sarkar *et al.*, 2006). Because of the considerable heterogeneity in aerosol sources and their relatively short residence time in the atmosphere, aerosols are always present in the atmosphere in extremely varying concentrations. Despite the fact that aerosols are always present in the atmosphere and have a wide range of sources, they cannot be viewed solely as a long-term offset to the warming impacts of greenhouse gases due to their short atmospheric residence duration (Harshvardhan, 1993). Depending on the ambient atmospheric conditions, aerosol optical properties, concentration, and size distribution, aerosols can either increase or decrease atmospheric heating over the monsoon region, causing a weakening or strengthening of the meridional temperature gradient and thus varying precipitation efficiency.

The majority of research has centered on aerosol variations in the seasonal mean climate, with sub-seasonal changes getting significantly less attention. We focused on sub-seasonal variations in aerosol characteristics and aerosol-induced radiative forcing during the monsoon in this study, with a particular emphasis on the transition phase of the monsoon because it is during this time that the seasonal reversal of the wind occurs, causing a massive influx of moisture and aerosols from the northern Arabian Sea and adjacent western arid regions. As the onset or beginning of the monsoon signals the commencement of the rainy season over the dry Indian subcontinent, any changes at the time of onset due to the induced aerosol radiative effect could be significant for the agriculture-based monsoon zone. Aerosols disrupt radiative fluxes within the atmosphere, possibly contributing in the thermodynamic structures of the atmosphere (Das *et al.*, 2015). Aerosols are most likely responsible for a substantial result of negative radiative forcing. Aerosol abundance is consistent over the Indian monsoon region, particularly during the wet monsoon, due to high transport and seasonal emission sources (Dave *et al.*, 2017), as a result, determining the impact of aerosols on radiative



transfer is difficult, because different aerosol types from different emission sources have different effects on radiation fluxes (short and long wave fluxes) and spectral distribution (AL-Taie *et al.*, 2020), which can have a significant impact on monsoon precipitation. Even modest variations in the onset, persistence, intensity and spatial distribution of monsoon precipitation can have disastrous implications in detecting and attribution of variability in the southwest monsoon is crucial.

The Indian monsoon region is a suitable site for conducting aerosol-monsoon interaction investigations due to major aspects such as spatiotemporal fluctuations in aerosol, cloud properties, rainfall, and topography. In addition, increased anthropogenic activities are linked to higher aerosol concentrations in the atmosphere in the current paradigm of industrialization and modernization; thus, aerosol physics is becoming more important in modelling. The SBDART model data that I we used in the study will provide a basic framework showing impact of aerosols on vertical atmosphere, therefore more regionalized studies on different space and time scales could produce more relevant or accurate outcomes. Therefore, a conceptual understanding of the large-scale monsoon circulation system predominantly during pre-monsoon to monsoon transition period over the Indian subcontinent can be gained by considering aerosol induced radiative forcing separately. The current research estimates:

- (i) Analyzing the spatial distribution of aerosols across the research area, as well as the relative contribution of aerosol species across the region
- (ii) The aerosol radiative forcing over the Indian monsoon region, as well as the regionalized forcing and accompanying heating rate in the atmosphere
- (iii) Regional impact of aerosol loading on precipitation in order to examine the aerosol-rainfall correlation.

## CHAPTER 2

### REVIEW OF LITERATURE

#### 2.1. AEROSOLS

Aerosols are microscopic particles suspended in the atmosphere that have the potential to cause significant changes in the earth's climate system by disrupting the radiation budget (Harshvardhan, 1993; IPCC, 2007; Manoj *et al.*, 2012; Bollasina *et al.*, 2013; Al-Salihi, 2018). Aerosols are a mixture of solid particles and the gas that holds them together in the atmosphere (Boucher & Olivier, 2015). The size distribution, chemical content, and form of the particles, all of which are highly variable in location and time, are the most essential properties of an aerosol population (Boucher & Olivier, 2015). Aerosol-induced solar dimming increases atmospheric stability and decreases convection potential by cooling the surface. (Sajani *et al.*, 2012). The aerosols can either enhance or curtail monsoon circulation thus affect the hydrological cycle (Ramanathan *et al.*, 2001). Although aerosols are a minor constituent of the atmosphere, their occurrence, residence time, physical properties, chemical composition, and corresponding complex refractive-index characteristics exhibit significant diversity, owing to wildly varying sources and formation processes, this can have a significant impact on the Earth's radiation budget, air quality and visibility, cloud formation, and cloud development (Ansmann & Müller, 2005). Large-scale circulation systems such as the Southwest monsoon, Hadley circulation, and Walker circulation are thought to have been influenced by changes in aerosol particle concentrations and distribution (Ekman, 2012), and aerosol concentration is, in turn, strongly dependent on certain meteorological parameters such as clouds, precipitation, and wind (Babu *et al.*, 2013).

Due to the extreme large heterogeneity in aerosol emission sources, including both natural and anthropogenic, and their relatively short residence time in the atmosphere, aerosols are always present in the atmosphere but in extremely variable concentrations. Aerosols are produced by natural sources such as wind-borne dust, sea spray, volcanic debris, biogenic aerosol, and anthropogenic

sources such as agricultural operations, fossil fuel combustion, waste and biomass combustion, and they exist in the atmosphere in a range of hybrid states including as externally mixed aerosols, internally mixed aerosols, coated aerosols, and most likely a combination of all of the above mentioned (Ramanathan, *et al.*, 2001). Aerosols have both local and non-local effects, which interact with one another. For example, during the onset phase of the monsoon, the local effect leads to the stabilisation and weakening of a developing monsoon depression over northeastern India and the northern Bay of Bengal, whereas non-local effects are primarily exerted through moisture and circulation feedback by enhancing low-level monsoon flow (Lau *et al.*, 2017).

## 2.2. AEROSOL TYPES

### 2.2.1. Absorbing and non absorbing types of aerosols

Aerosols can be classified into two categories based on their absorbing properties: those that absorb solar radiation and those that do not (Kumar *et al.*, 2016). Aerosols interact with incoming electromagnetic radiation in one of two ways: they either scatter the radiation in all directions anisotropically, which is known as scattering or they absorb the energy and convert it to heat, which is known as absorption (Boucher & Olivier, 2015). Absorbing aerosols, such as dust and black carbon, are well known for their ability to warm the atmosphere by absorbing solar radiation, and thus to counterbalance cooling effects caused by reflective aerosols such as sea salt and sulfate (Sivan & Manoj, 2019). Dust's thermal effects are complex and vary depending on vertical distribution; for example, dust in the stratosphere reflects incoming solar radiation and cools the surface, whereas dust in the lower troposphere can contribute to surface warming by absorbing both incident and outgoing solar radiation (Collier and Zhang, 2008). In contrast, non-absorbing aerosols such as organic carbon and sulphate scatter solar radiation and have a relatively weak atmospheric heating effect (Collier and Zhang, 2008). Both absorbing and non-absorbing aerosols scatter sunlight and lessen the amount of solar radiation reaching the Earth's surface, resulting in a negative forcing effect referred to as solar dimming. (Lau and Kim, 2006). The chemical composition, size distribution, and number density

all influence the scattering and absorption of solar light by aerosols, among the chemical composition determine the refractive index (Ramanathan, *et al.*, 2001).

### **2.2.2. Aerosols from surface source and spatial source**

Jaenicke (1993) divided atmospheric aerosols based on their sources: extensive surface sources such as oceans and deserts, and spatial sources such as gas to particle conversion (GPC) and clouds. Aerosol properties vary spatially; they can be classified as urban, semi-urban, continental, desertic, marine, volcanic, or stratospheric aerosol layers of the atmosphere; however, this is an inexact classification because aerosols could even travel a long distance and therefore is not always representative of the spot where they can be found; thus, a broad category is required (Boucher & Olivier, 2015).

### **2.2.3. Natural and anthropogenic aerosols**

Aerosols arise from a wide range of emission sources mainly distinguished as natural and human-made sources or anthropogenic sources, referred as natural and anthropogenic aerosols having extremely varied size and space–time distributions (Rizza *et al.*, 2019). Dust, sea salt, smoke, Black carbon (BC), and (OC) from forest fires, biogenic and biological particles, are examples of natural aerosols (Lau *et al.*, 2008). Sea salt produced by physical process over the ocean especially through breaking or bursting of waves or bubbles, mineral dusts are blusted from the surface by the action of wind, and organic aerosols produced by biogenic emissions are all natural sources of aerosols (Harshvardhan, 1993). Artificial, or anthropogenic, aerosols include sulfate, nitrate, and carbonaceous aerosols, which are mostly produced by activities such as large-scale biomass burning, transportation, cement manufacturing, metallurgy, waste incineration, and so on. (Harshvardhan, 1993; Babu *et al.*, 2013). Cloud droplets of various sizes can be attributed to the higher concentrations of anthropogenic aerosols with various chemical compositions and sources (Kumar *et al.*, 2016). The principal anthropogenic components of tropospheric aerosols are sulphate, BC, OC, mineral dust, and nitrate aerosol (Haywood & Boucher, 2000).

#### 2.2.4. Primary and secondary aerosols

Aerosols are classified into primary and secondary categories based on their production processes and chemical composition. Carbonaceous aerosols, by-products of combustion products processes, wind-blown mineral dust aerosols, and sea salt from the sea floor are examples of primary aerosols that are directly discharged into the atmosphere (Harshvardhan, 1993; Babu *et al.*, 2013). Aerosols formed by the mechanical action of wind friction on an oceanic or terrestrial surface, as well as aerosols produced during incomplete combustion, have been ejected as minute particles into the atmosphere. Secondary aerosols, on the other hand, are produced by gas-to-particle conversions and aqueous phase oxidation pathways. (Bellouin & Haywood, 2015; Haywood & Boucher, 2000). Secondary aerosols are particles that are formed by the by the process of condensation by atmospheric gas-phase species, which can undergo a number of chemical transformations before condensing, rather than being emitted directly into the atmosphere as particles (Boucher & Olivier, 2015).

#### 2.2.5. Nucleation mode, ultrafine mode, or coarse mode

Aerosols are classified as nucleation mode, ultrafine mode, or coarse mode based on the size of their particles. Nucleation mode describes aerosol particles with diameters less than 0.1  $\mu\text{m}$ , ultrafine mode describes particles with diameters less than 0.01  $\mu\text{m}$ , and coarse mode describes particles with diameters greater than 1.0  $\mu\text{m}$ . (Shaeb, 2019). These particles can stay in the atmosphere for 1–7 days (boundary layer), 3–10 days (free troposphere), and 1–365 days (stratosphere) and conduct long-distance transit during that time (Shaeb, 2019).

### 2.3. SOURCES AND SINKS

Because of the chemical features of aerosols, they can persist in the atmosphere for a variety of lengths, referred to as residence time, which can range from 1-2 weeks (Boucher & Olivier, 2015). A simple equation can be used to compute the residence duration ( $t$ ) of aerosols in the atmosphere:

$$t = \frac{B}{S} = \frac{B}{R} \quad (\text{Equation 1})$$

B signifies the aerosol load or vertically integrated aerosol column in the atmosphere, S the source flux, and R the removal (sink) flux (Boucher & Olivier, 2015). Aerosols can be emitted from a variety of sources, including marine, volcanic, biomass burning, deserts, and biogenic surfaces, and the principal two sinks of aerosols are dry deposition, wet deposition (Boucher & Olivier, 2015) and gravitational settling. Wet deposition is the removal of aerosols by precipitation occurs in and below the clouds, while dry deposition is the removal of aerosols by interacting with the earth's surface by impaction (Haywood & Boucher, 2000; Lau *et al.*, 2017). Arya *et al.*, 2021 discovered that aerosol residence time was longer during break conditions than in normal conditions, potentially increasing aerosol loading over India

## 2.4. MAJOR AEROSOL SPECIES

### 2.4.1. Dust

On a global basis, dust plays the most important role (IPCC, 2007). Deserts, dry lake beds, semi-arid deserts, and other types of dust sources are more common in the northern hemisphere than in the southern hemisphere (IPCC, 2007). Dust can absorb solar radiation and generate local heating, changing the relative humidity and stability of the atmosphere and thus influencing cloud lifetime and cloud liquid water content. The radiative property of dust aerosol is determined by its vertical height as well as the ambient condition in which it exists; e.g., dust in the stratosphere generally contributes to surface cooling by reflecting incoming solar radiation, whereas dust in the lower troposphere can contribute to surface warming by absorption of solar radiation and outgoing longwave radiation from the surface (Collier & Zhang, 2009). Depending on where the aerosol layer is located, dust can either stabilise or destabilise the boundary layer; for example, dust over arid and semiarid regions is likely to evaporate clouds when aerosols with a high water content are present (Chung & Ramanathan, 2006). The main parameters that influence dust aerosol emission are wind speed and soil conditions. Human-caused land surface change can also have a considerable impact on dust emission. Natural dust aerosols can aid deep convection by acting as condensation nuclei and can also stabilise the atmosphere by its property of

absorbing by semi-direct effect over monsoon regions (Lau *et al.*, 2008). The elimination of atmospheric dust aerosol is caused by the combined impact of scavenging and dry deposition (Grandey *et al.*, 2018). The lifetime of dust is determined by size of aerosol particles; coarse particles are readily eliminated from the atmosphere by gravity settling, whereas sub-micron particles can have a prolonged atmospheric lifetime. Grandey *et al.* (2018) used the CAM5.3-MARC-ARG model, which is a new configuration of the Community Atmosphere Model version 5.3 (CAM5.3), to determine the lifetime of major aerosol species in the atmosphere.

According to his research (Grandey *et al.*, 2018), dust aerosols have a lifespan of 3-4 days. During the pre-monsoon period, dust was identified as the most common type of aerosol, which can scatter and absorb incoming solar radiation, increasing atmospheric heating, increasing atmospheric stability, and altering cloud formation and distribution (Dipu *et al.*, 2013). The direct radiative effect of dust is calculated by taking into account the effects of all anthropogenic and natural dust aerosols on radiative flux at the top of the atmosphere, at the surface, and within the atmosphere, as determined by aerosol optical properties such as aerosol optical depth (AOD), extinction coefficient, single scattering albedo (SSA), and asymmetry parameter (Galleria & Kuniyal, 2016).

#### **2.4.2. Black carbon (BC)**

BC aerosols emitted by incomplete hydrocarbon combustion, such as those emitted by combustion engines, coal-fired power generation, slash-and-burn farming techniques, and cooking fumes etc. (Lau *et al.*, 2008). BC is well known to counteract the cooling effect produced by scattering-type of aerosols like sea salt and sulfate due to absorptive nature (IPCC, 2007). During the pre-monsoon months, the entrainment of black carbon aerosols over the elevated slopes of north-central India scatters and absorbs solar radiations, causing an increase in heating rate (Lau & Kim, 2006).

### **2.4.3. Organic carbon (OC)**

The incomplete combustion of organic matter and biomass, produces carbonaceous aerosol called organic carbon which contain compounds of carbon, hydrogen and oxygen and operationally scattering in nature (Boucher, 2015) or formed as secondary aerosol particles from condensation of organic gases considered semi-volatile or having low volatility (Contini *et al.*, 2018). it is one of the most significant contributors to particulate matter mass concentrations, coming from both anthropogenic and natural sources such as biofuel and fossil fuel combustion processes, sea-spray and biogenic emissions and are removed from the atmosphere by impaction scavenging (Contini *et al.*, 2018; Grandey, *et al.*, 2018)). Organic carbon has a mass concentration 3–12 times that of BC in atmospheric aerosol, and it is one of the main drivers of the oxidative potential of atmospheric particles due to its high solubility ( Zhang *et al.*, 2017). The lifetime of organic carbon aerosol is approximately 5 days (Grandey, *et al.*, 2018).

### **2.4.4. Sulfate**

Chemical processes in the atmosphere produce sulfate aerosols from gaseous precursors, anthropogenic sources, volcanoes, biogenic sources, and other sources (IPCC, 2007). The sulfate aerosols scatter the incident radiation thus enhances surface reflectivity causing the weakening of land-sea thermal contrast and affect the Indian monsoon (Mitchell & Johns, 1997). The strength of the source, the velocity of chemical transformation, and the fraction of precursors eliminated before the conversion process all influence the creation of sulfate (IPCC, 2007). The primary sink of sulphate aerosol is nucleation scavenging by stratiform clouds; however, scavenging does not always imply permanent removal from the atmosphere due to hydrometeor evaporation. (Grandey, *et al.*, 2018). The atmospheric persistence of sulphate aerosol is few days to a week (Grandey, *et al.*, 2018).

### **2.4.5. Sea salt**

Sea salt aerosol are produced by a variety of mechanisms, including the bursting of air bubbles during whitecap development, indicating that simulated



wind speed and sea surface temperature have a strong influence on sea salt formation. (IPCC, 2007; Grandey *et al.*, 2018). Because sea salt is regarded as an effective CCN, characterizing its surface production is critical in investigating aerosol indirect effects (IPCC, 2007). Sea salt particles are very minute particles ranges from 0.05 to 10  $\mu\text{m}$  in diameter and have wide range of atmospheric residence times ranging from 0.6 to 0.8 days (IPCC, 2007; Grandey *et al.*, 2018). The major sinks that remove aerosol from the atmosphere are dry and wet deposition (Grandey *et al.*, 2018). Boucher (2015) referred the sea salt aerosol as sea spray aerosols by considering the possibility that it may also contain biological material and other contaminants.

## 2.5. MAY-JUNE TRANSITION PHASE

The May-June transition is critical in defining aerosol forcing and the subsequent reaction and feedback of the hydrological cycle because it is during this time that aerosols begin to accumulate over the Indian core monsoon region, primarily over the Indo-Gangetic basin, and may determine when and where wash-out occurs (Lau *et al.*, 2006). During transition phase, the aerosol direct forcing appears to be the dominant factor, while the direct radiative forcing found to more significant during May and become modest during June (Bollasina *et al.*, 2013). Aerosols found to be the primary cause of a positive trend in precipitation rate over central and northern India during the transition phase, indicating an earlier monsoon onset, which was then significantly reduced for the rest of the summer monsoon period, according to the study led by Bollasina *et al.*, (2013).

## 2.6. COMPLEX NATURE OF AEROSOLS

Aerosols in the atmosphere are one of the main underlying factors in controlling the thermodynamic state of the atmosphere, which controls convection, cloud development, cloud lifetime, and precipitation (Al-Salihi, 2018). Because aerosols have considerable uncertainty in their size and concentration in both spatial and temporal distribution, there's a potential that forcing and temperature response will alter quickly and locally, which implies their complex nature of interactions (Ekman, 2012). Aerosols have a wide range

of microphysical and dynamical effects due to changes in their optical properties, concentration, and high spatial and temporal distributions, which have a variety of effects on the emission spectrum of radiation (Das *et al.*, 2015). Aerosol particles have most likely made a significant negative contribution to overall radiative forcing, but due to their short atmospheric lifetimes, they cannot be used simply as a long-term offset to the warming influence of greenhouse gases, making quantifying aerosol radiative forcing more difficult than quantifying greenhouse gas radiative forcing (IPCC, 2007). On a global scale, aerosol induced solar dimming reduces land-sea thermal contrast and weakens the monsoon meridional circulation and, on a local scale, aerosol radiative forcing alters the thermodynamic stability of the lower atmosphere resulting in reduced convective potential and, weakened wind and atmospheric circulations (Li *et al.*, 2016). Fine sized particles scatter more radiation per unit mass and have a longer air residence time than coarser particles, hence their size distribution is important in determining direct radiative forcing, and as a result, it's critical to know the processes that determine these properties (IPCC, 2001). The complexity of the aerosol-monsoon interaction at various space-time scales is more complex to address due to a combination of microphysical and dynamical consequences of aerosol radiative forcing, as well as meteorological forcing (Das *et al.*, 2015). In particular, the first and second indirect impacts have a negative forcing on climate, whereas the invigoration effect and semi-direct effect have a positive forcing, making it difficult to accurately measure those opposing effects (Huang *et al.*, 2014).

## 2.7. HOW TO MEASURE AEROSOL PROPERTIES?

Measurements from the ground, space, and air-bound platforms are the three basic platforms that have been established for the regular and timely study of understanding aerosols (Onyeuwaoma *et al.*, 2018). Models are validated using ground-based measurements because the derived aerosol properties provide a foundation for validating atmospheric correction procedures (Verma *et al.*, 2019). However, there's a risk that these particles will be transmitted and accumulated far

from their source and surveillance stations, making aerosol supervision more difficult (Onyeuwaoma *et al.*, 2018). Point data from sunphotometer-equipped ground locations, on the other hand, has the highest accuracy (Verma *et al.*, 2019). For monitoring aerosols, various ground-based instruments are used, including spectroradiometers, which provide excellent spectral performance across the entire solar irradiance spectrum, multichannel radiometers, and broadband radiometers, which provide wavelength integrated quantities and are more widely used because they are less expensive than spectroradiometers (Verma *et al.*, 2019). Satellite-based remote sensing instruments are widely used because satellite remote sensing data has a high spatial and temporal resolution, making it a valuable source of information about aerosols in most atmospheric studies to predict future climate (Kaskaoutis *et al.*, 2010; Verma *et al.*, 2019). The ozone monitoring instrument (OMI) is a device that measures the amount of aerosols in the atmosphere, as well as classifying them and measuring cloud pressure and coverage (Verma *et al.*, 2019). Multi-angle imaging spectroradiometer (MISR) which can detect the amount and type of aerosol particles produced by natural and anthropogenic activities, as well as the type and height of clouds, and identify land surface types (Verma *et al.*, 2019). Moderate resolution imaging spectroradiometer (MODIS) measure different aerosol optical properties, such as AOT, types of aerosols, and aerosol size-distribution, on the earth's surface every 1–2 days, allowing to better demonstrate complex atmospheric physical processes and changing climate dynamics over land and oceans (Verma *et al.*, 2019).

## 2.8. AEROSOL RADIATIVE FORCING

Aerosol radiative forcing is the effect of aerosols interacting with solar radiation, either directly or indirectly, to change the earth's energy budget, altering global temperature and associated internal fluctuations in the climate system (Ramachandran and Cherian, 2008). Aerosol radiative forcing is defined as a change in radiative fluxes caused by aerosols at the surface or at the top of the atmosphere that alters the net energy balance (Ramanathan *et al.*, 2001). However, due to the lack of a comprehensive global database of aerosol

concentrations, inhomogeneity in occurrence with respect to time and space, and inherent characteristics such as chemical composition and optical properties, this is difficult to quantify (Ramanathan, *et al.*, 2001). The major factors determining the effect of radiative forcing are surface albedo, SSA, and asymmetry parameter (Pandithurai *et al.*, 2004). Because of substantial spatial uncertainties, the local estimates of aerosol-induced mean radiative forcing may exceed the global values (Pandithurai *et al.*, 2004). Bollasina *et al.* (2013) discovered that the aerosol produced forcing spreads westwards and reaches a maximum value of  $-16\text{W/m}^2$  over the Bay of Bengal in May, and that the forcing increases further in June, resulting in greater air stability (Figure S5) and reduced precipitation. Anthropogenic aerosols almost certainly create a net negative radiative forcing (cooling influence) in the NH that is larger than in the SH, the increased loading of aerosol reduce the amount of electromagnetic radiation reaching the surface and has a greater impact on precipitation and other components of hydrologic cycle (IPCC, 2007; Ramanathan *et al.*, 2001). The total radiation lost to space for the earth-atmosphere system is given by the aerosol radiative forcing at the TOA forcing, which is always lesser than the surface radiative forcing due to the absorption and redistribution of incoming solar radiation inside the atmosphere (Rajeev & Ramanathan, 2002). Although the global direct aerosol radiative forcing is negative, due to their changes in optical properties that are determined by their mixing state, size disposition, and chemical composition aerosols can cause either negative or positive forcing for the atmosphere (Ramanathan, *et al.*, 2001; Sivan and Manoj, 2019). There are three primary mechanisms by which aerosols interact with radiation, which are listed below:

### **2.8.1. Direct radiative forcing**

Aerosols primarily interact directly by reflecting and absorbing shortwave radiation and by absorbing and emitting some longwave radiation (Collier & Zhang, 2008; Corrigan *et al.*, 2006). Both the scattering and absorption is influenced by the particle size, hygroscopic growth, concentration and particle concentration (Corrigan *et al.*, 2006). The single scattering albedo, SSA, is the ratio of scattering to the sum of scattering and absorption, and it is an important

indicator for assessing a particle's relative scattering and absorption (Ramanathan *et al.*, 2001). The value of SSA ranges from 0 to 1, aerosols that are close to 1 are scattering types of aerosols causing negative TOA forcing and values close to 0 are absorbing-type causing positive TOA forcing. SSA is a wavelength parameter factor that determines the cooling and warming effect of aerosols (Kant *et al.*, 2015). Sulfate, sea salt, and nitrate have SSA values close to 1, suggesting that they are scattering aerosols, whereas black carbon, dust, and smoke have SSA values close to 0, implying that they are absorbing aerosols (Ramanathan *et al.*, 2001; Sivan & Manoj, 2019).

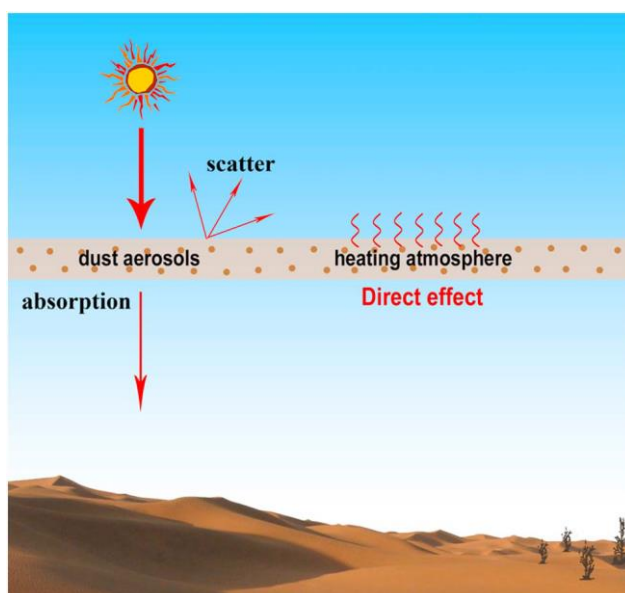


**Figure 1: Schematic depiction of the direct radiative effect of aerosols. Adapted from “Climate effects of dust aerosols over East Asian arid and semiarid regions” by, Huang *et al.*, 2014.**

### **2.8.2. Indirect radiative forcing**

Aerosol particles can function as cloud condensation nuclei; their efficiency is determined by their size and water response, i.e., atmospheric aerosol particles are either hydrophobic or hydrophilic (Babu *et al.*, 2013). Only particles with specific water-soluble species are influential for indirect forcing because they have hydrophilic sites that allow them to moisten and activate at higher supersaturations (Babu *et al.*, 2013), whereas CCN greatly influences cloud reflectivity, cloud lifetime, and precipitation rate (Kant *et al.*, 2015). Aerosols interact

indirectly by modifying the microphysical properties of cloud liquid water content, cloud fraction, cloud top temperature, droplet number concentration, cloud particle size through altering cloud albedo and lifetime which are proposed by Twomey (1977) and Albrecht (1989). Using ground-based measurements Kumar *et al.* (2016) reported that the AIE is highest in clouds with low liquid water content, while the dispersion of cloud droplet size distribution is substantially lower. The ‘Twomey effect’ or ‘cloud albedo effect’ or ‘first indirect effect’ refers to the radiative impact where an increase in aerosols reduces the cloud droplet effective radius, whereas the ‘Albrecht effect’ or ‘cloud lifetime effect’ or ‘second indirect effect’ increases the concentration of cloud condensation nuclei, thereby enhancing the cloud amount, and thus enhancing the cloud lifetime, and reduces the rate of collision coalescence, results in a delay in onset of precipitation (Collier & Zhang, 2008; Corrigan, *et al.*, 2006).

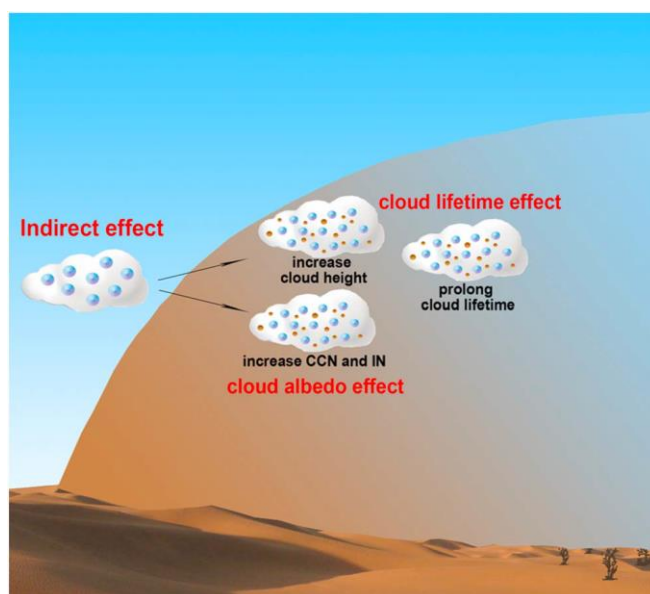


**Figure 2: Schematic depiction of the indirect radiative effect of aerosols. Adapted from “Climate effects of dust aerosols over East Asian arid and semiarid regions” by, Huang *et al.*, 2014.**

Twomey *et al.* (1977) argued that any increase in the number of cloud condensation nuclei, if either natural or anthropogenic, could have a significant impact on cloud microphysics by increasing cloud reflectivity. The Twomey effect

describes a raise in aerosol number concentration that can cause more cloud drops to form, brighten the clouds, and exert a negative forcing. Because of the Twomey effect, the aerosols released by biomass burning increase CCN concentration, which reduces spectral dispersion and thus increases cooling (Martins & Dias, 2009). The first indirect effect is a reduction in cloud effective radius caused by an increase in CCN concentration associated with an increase in aerosol loading, while the aerosol dispersion effect partially offsets the reduction in droplet radius, resulting in a positive correlation between CCN and effective radius (Kumar *et al.*, 2016; Martins & Dias, 2009; Panicker *et al.* 2010).

According to the Albrecht effect, if the liquid water content inside the cloud is unaffected by increased aerosol concentration, the amount of cloud condensation nuclei (CCN) in the atmosphere will increase, resulting in more, but smaller, cloud droplets that will take longer to grow to sizes that can easily fall as precipitation (Ramanathan *et al.*, 2001). During the summer monsoon season, aerosol abundance is persistent throughout the Indian subcontinent and has a substantial impact in cloud microphysical properties, which have been linked to both precipitation suppression and invigoration at various aerosol levels (Dave *et al.*, 2017).

### **2.8.3. Semi-direct radiative forcing**

In addition to the indirect and direct cooling effects of aerosols, there is a significant third way in which aerosols can influence climate, known as the semi-direct effect, in which light-absorbing aerosols warm the atmosphere relative to the temperature of the surface, reducing the upward movement of moisture and, as a result, reducing cloud cover (Hansen *et al.*, 1997). Due to their property of absorbing solar radiation, absorbing aerosols such as dust and black carbon generate local heating within the troposphere, which can influence cloud formation and development by changing environmental conditions such as relative humidity and atmospheric stability (Huang *et al.*, 2014). Changes in cloud cover may also occur as a result of the semi-direct effect, as it may warm clouds, increasing evaporation of cloud droplets and thus reducing cloud water path

(Huang *et al.*, 2014). According to Hansen *et al.*, 1997 aerosols with single scatter albedo as high as 0.9 can result in a net positive climate, owing to a semi-direct cloud effect that reduces large-scale cloud cover in layers with absorbing aerosols. The semi-direct effect is thus likely to be heavily influenced by local atmospheric conditions, the vertical location of the aerosol layers relative to the inversion, and, most importantly, the presence of absorbing aerosol material, for example, absorbing aerosol above the boundary layer increases the liquid water path, resulting in a negative semi-direct forcing (Johnson *et al.*, 2003). Lohmann and Feichter (2001) used the ECHAM4 general circulation model to investigate the global impact of black carbon (BC), an important absorbing type of aerosol. They uncovered that BC absorption occurs only in clear air and results in zonal mean reductions in cloud cover and liquid water path in highly polluted regions of the Northern Hemisphere.

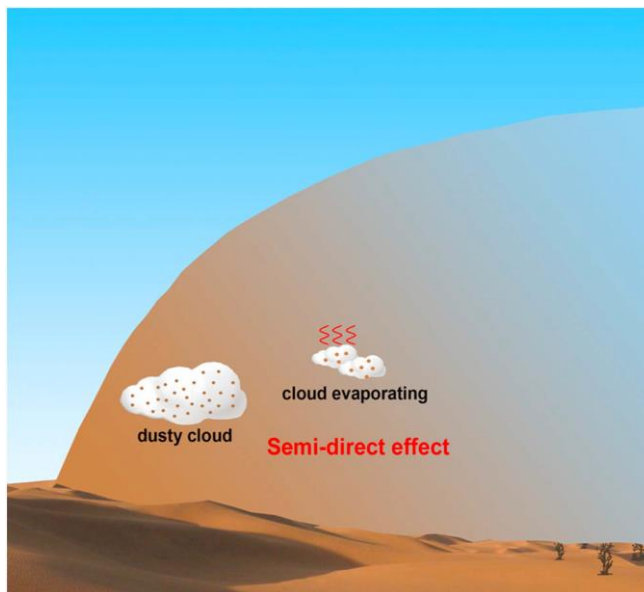


**Figure 3: Schematic depiction of the direct semi-radiative effect of aerosols. Adapted from “Climate effects of dust aerosols over East Asian arid and semiarid regions” by, Huang *et al.*, 2014.**

## 2.9. AEROSOL AND GREENHOUSE GASES

- In general, both aerosols and greenhouse gases influence the energy budget and hydrological cycle; however, the aerosol radiative forcing is comparable to that



caused by greenhouse gases on a global scale, but with the opposite sign (Rajeev & Ramanathan, 2002)

- Greenhouse gas emissions are uniformly distributed over the planet, but aerosols are highly heterogeneous in terms of space and time (Kaufman *et al.*, 2002), resulting in differences in their physical and chemical properties, and they are regionally distributed (Rajeev & Ramanathan, 2002)
- Because green house gases have a lengthy residence period in the atmosphere (up to 100 years) compared to aerosols, which only stay in the atmosphere for a week, the warming caused by green house gases cannot be compensated by surface cooling caused by aerosols particles (Kaufman *et al.*, 2002)
- Greenhouse gases absorb a portion of longwave radiation that scatters or reflects back to space, resulting in net surface warming, whereas aerosols scatter and reflect incident radiation, resulting in a dimming effect, leading to a substantial surface cooling (Kaufman *et al.*, 2002)

#### 2.10. SOURCE REGIONS OF AEROSOLS

In northern India, especially in the Indo Gangetic plains, anthropogenic emissions, primarily black carbon (BC) and sulfate aerosols, are abundant throughout the year (Kumari *et al.*, 2007). Aerosol "hotspots," or regions with high natural and anthropogenic aerosol concentrations, have been spotted over the Indo-Gangetic Plain in East Asia, the Sahara desert in South Africa, and the Amazons in South America, all of which are clearly linked seasonally and geographically to major monsoon regions. Using the GOCART model, Lau *et al.* (2017) estimated that desert dust transmitted from the Middle East deserts and the Thar desert of the northern Indian subcontinent provides a significant fraction of the AOD over the Arabian Sea, northwestern and northern India.

#### 2.11. AEROSOL LOADING OVER INDIA

The periodic cycle of wet (southwest) and dry (northeast) monsoon with a pattern that changes generally for every 6 months from southwest to northeast or vice versa allows for a variety of aerosol deposition and characteristics over the Indian subcontinent (Ramachandran & Cherian, 2008). During the wet monsoon,

the strong and moist southwest wind brings clean air from the Southern Hemisphere into the monsoon region, whereas the dry monsoon brings polluted air from Asia (Corrigan *et al.*, 2006). During winter (December-February), the calm low-level synoptic winds from the polluted northern hemisphere bring mostly anthropogenic aerosols to the Indian subcontinent, whereas during pre-monsoon (March-May), the westerlies travel through less polluted west, bringing mineral dust from the adjacent Thar desert and the Middle East to western India, and during monsoon (June-September), the westerlies get intensified further and during post-monsoon the wind pattern shift from southwest to north east (Ramachandran & Kedia, 2013). Over northern India two branches of AOD can be distinguished (i) southern division over the Gangetic plains of the southern slope of TP where carbonaceous aerosol emitted from industrial activities as well as biomass combustion from northwestern India and Pakistan is abundant during the pre-monsoon period (March–April) and considerably reduced during the transition period (May–June) due to wet deposition (ii) the northern section, the aerosol consists primarily of dust transported from the Taklamakan Desert builds up over the northern slope of TP in March–April, peaks in May–June and begins to drop towards winter (Lau *et al.*, 2006). Guleria & Kuniyal (2016) analyzed the spatial variations in aerosol distribution with respect to changing seasons, finding that the consequence of aerosol was higher over the northeastern part of India and the Indo Gangetic Plain (IGP) during the premonsoon season compared to the rest of the seasons, whereas the effect was higher over the southern and eastern coastal regions of India during winter and the effect was higher over the southern and eastern coastal regions of India. Dave *et al.* (2017) examined the aerosol burden during break periods across India and discovered that the aerosol-induced inhibition of precipitation seen in the study is due to mesoscale atmospheric stabilization over short time intervals of 3–5 days. It has been discovered that during the phase change from active to break spell over central India, the circulation pattern shifts from moist dynamic-low to drier heat-low, which is exemplified by intense heating at the surface and weak ascent, which also enhances transport of large amounts of aerosol from the west along with

westerlies and gets trapped in the lower atmosphere because of the large scale subsidence (Arya *et al.*, 2021). It has been observed that fine mode aerosols dominate over the Indo Gangetic plain during the post-monsoon, but coarse mode particles dominate during the premonsoon (Kedia *et al.*, 2014). The topography of northern India especially the foothills of Himalaya with complex and steep topography favors the accumulation of desert dust from the arid- semiarid regions across Arabian sea and accumulated over northwestern and central India (Lau *et al.*, 2017). Mineral dust was noticed to be a major aerosol type found over the IGP, which is primarily transported from deserts in western India, Pakistan, and the Middle East, implying the importance of large scale circulation (Lau *et al.*, 2008). In turn, the anomalous large scale circulation during the monsoon causes changes in aerosol forcing by modulating the amount of transport, removal mechanisms, physical and chemical nature of aerosols, and leads to changes in the hydrological cycle through interaction with cloud microphysical properties (Lau *et al.*, 2008). Dust events over the Sahara Deserts that begin around March–April and culminate around August–September have been observed to play a significant role in causing a heap of aerosols over the Indian subcontinent during the summer monsoon, causing maximum surface forcing over India in the months June–July (Sarkar *et al.*, 2006).

## 2.12. TRENDS IN AEROSOLS

Trends in aerosols Murthy *et al.*, (2013) conducted a trend analysis of aerosol load using the AOD spectral index over the Indian subcontinent from 1986 to 2011 and discovered that, on average, the aerosol optical depth increases at a rate of 2.3 percent per year, owing to an increase in anthropogenic proportion. Over the previous five decades, there has been a massive change in aerosol loading across India, which has been linked to a large increase in population and increasing urbanization (Moorthy *et al.*, 2013). The amount of natural and anthropogenic aerosols discharged into the atmosphere has been steadily increasing as a result of diverse and contrasting geographical features, high population density, and anthropogenic activities associated with modernization,

urbanization, and industrialization, and linked rapid economic development, which can have a significant impact on synoptic meteorological conditions over the Indian monsoon region associated with the southwest monsoon (Moorthy *et al.*, 2013). According to Babu *et al.*, (2013), an insignificant trend in AOD observed over the Indo-Gangetic Plain (IGP), a regional hotspot of aerosols, during the pre-monsoon and summer monsoon seasons is primarily attributed to the combined effects of dust transport and wet removal of aerosols associated with monsoon rainfall, both of which are highly variable interannually. Using data from long-term spectral AODs recorded from a network (ARFINET) of observatories dispersed across India, statistically significant and persistent increasing patterns in AOD were noticed mostly contributed by anthropogenic emissions were assessed (Babu *et al.*, 2013). There exist a regular cycle of absorbing aerosols, notably dust over the IGP, which peaks from February to May and then rapidly falls in June and July when monsoon rains begin, with a subsequent peak in October (Bollasina *et al.*, 2008). Monthly mean of AOD over the Arabian Sea has a distinct annual cycle, with a maximum during the summer monsoon compared to those over the Bay of Bengal, peaking in July, and a minimum during the winter, dipping to its lowest level in January (Lau *et al.*, 2008). The transport of mineral dust from the western desert by westerly winds at and above 700 mbar, the enhancement of sea salt production by the impact of strong westerly winds, and the high humidity of the south westerly surface winds were found to be the major three reasons for the high aerosol burden (Lau *et al.*, 2008).

### 2.13. AEROSOL MONSOON INTERACTION

Interannual variability in Indian monsoon rainfall is primarily due to thermodynamic adjustments of mean temperature, moisture content, zonal wind, and dynamic circulation adjustments, all of which are heavily influenced by external factors such as sea surface temperature (SST), soil moisture, snow cover, atmospheric aerosols, El Nino Southern Oscillation, and Indian Ocean Dipole (Ramachandran & Kedia, 2013; Dave *et al.*, 2017), among aerosols play significant role (Ramachandran & Kedia, 2013). Changes precipitation linked to

aerosol abundance, occur as a result of thermodynamic adjustments, which can result in either an increase or decrease in meridional surface temperature, causing a surge or decline in northward moisture transport, and thus the onset or delay of monsoon precipitation on time scales of days to months (Dave *et al.*, 2017).

Increased aerosol concentration changes the intensity of solar radiation directly by scattering radiation back to space and absorbing radiation in the atmosphere, resulting in a decrease in cloud effective radius and thus an increase in cloud albedo and cooling of the climate system, resulting in differential cooling of the source and non-source locations and a decrease in the land-sea temperature gradient leading to weakening of monsoon circulation (Ramachandran & Kedia, 2013). The main mechanisms for monsoon circulation weakening (strengthening) were found to be aerosol-induced differential cooling (heating) of the source and non-source areas, as well as a limitation (enhancement) in the land-surface thermal contrast (Ramachandran & Kedia, 2013). The significant impact of aerosol solar heating on the atmosphere functions as a significant positive forcing on the monsoonal circulation, resulting in considerable interannual and intraseasonal variability in precipitation (Goswami & Xavier, 2003; Manoj *et al.*, 2011; Chung & Ramanathan, 2006).

Aerosol in the atmosphere influences weather predictability by modulating the frequency of synoptic events like lows, depressions, and tropical cyclones, as well as controlling seasonal mean climate and event-to-event variability of the monsoon intraseasonal oscillations (Manoj *et al.*, 2012). During the pre-monsoon season (March-April-May (MAM)), low level westerlies begin to blow from/through a less polluted west (arid/marine) and carry mineral dust from the neighbouring Thar Desert and the Middle East. Using the evidence from MODIS satellite data Krishnamurti *et al.* (2013) point out that summer levels of aerosol optical depth (AOD) are comparable or even higher compared to the drier seasons and could have possible impacts on monsoon convection and associated monsoon depressions. The study result Grandey *et al.*, (2018) found that relative humidity and wet scavenging are important drivers of the precipitation-aerosol concentration relationship. Collier and Zhang (2008) used the NCAR Community

Atmosphere Model (CAM3) and the Goddard Global Ozone Chemistry Aerosol Radiation and Transport Model (GOCART) to show that adding aerosols during pre-monsoon periods to the atmosphere destabilises the atmosphere allowing for increased convection and precipitation and, accordingly, has a negative feedback on precipitation during the active monsoon months of June and July.

Manoj *et al.* (2012) investigated the indirect effect of aerosols on the event-to-event variability of the monsoon intraseasonal oscillations (ISOs), and showed that the impact of forcing will be regionally diverse throughout the same time period. Despite wet deposition, adequate aerosol optical depth remains over India during the summer months, according to Krishnamurti *et al.* (2013), because pollution steadily makes up from surface emissions. Das *et al.*, (2015) observed that aerosols tend to boost the summer monsoon zonal mean wind at 850 hPa across the IGP where there is greater spatial coverage of aerosols, but have no effect on the corresponding mean meridional wind component. Changes in vertical wind shear, zonal and meridional circulation, and, most significantly, advection are all linked to aerosol-induced heating (Das *et al.*, 2015), indicating that aerosol-induced solar heating offers a diabatic heating source for rising motion over NIO and India (Chung & Ramanathan, 2006).

Li and Ramanathan (2002) calculated the variation in AOD over the tropical Indian Ocean during the transition from winter to summer monsoon season, finding that there are large seasonal variations in AODs modulated by the monsoons, with aerosol distribution over the Arabian Sea displaying a strong annual cycle maximum in summer months and a minimum in winter, whereas AODs over the Bay of Bengal exhibited a weak annual cycle with both maximum and minimum during the transition from winter to summer. According to the findings of Bibi *et al.* (2017), coarse mode aerosols were more prevalent in the summer and pre-monsoon seasons, while fine sized aerosol were more prevalent in the winter and post-monsoon seasons, and thus SSA were found to be higher during the summer and pre-monsoon seasons, which is due to the influence of coarse absorbing particles.

### 2.13.1. The solar dimming effect

Aerosols, which are microscopic particles in the atmosphere that form as a result of natural and human-made activity, have a massive effect on incident solar radiation that falls on the earth's surface (Kumari & Goswami, 2010). The solar dimming effect, which is caused by the scattering or absorption of solar radiation by both absorbing and non-absorbing aerosols, causes surface cooling due to the insulation of solar radiation reaching the surface (Lau & Kim, 2006; Lau *et al.*, 2006). Surface dimming and atmospheric heating values range from 10% to 20% of the latent heating of the atmosphere and surface evaporation, according to Lau *et al.*, 2008. Aerosols function as cloud condensation nuclei, hence rise in aerosol load might result in more cloud formation with small drop sizes, brightening the cloud and increasing cloud albedo, which would tend to reflect even more incoming sunlight back into space (Kumari & Goswami, 2010). Surface cooling induced by aerosols is stronger over land, where aerosol sources are located, than over the oceans, reducing the land–ocean temperature differential and weakening monsoon overturning (Lau, 2016). Because the emission sources are mostly located over the land surface, the dimming caused by aerosols is more pronounced over the land than over the ocean (Lau, 2016). The increased aerosol burden of sulphate (strong scatterer) and black carbon (strong absorber) owing to changing patterns of anthropogenic emissions contribute around one-third of global average optical depth and are likely contributing to solar dimming (Kumari *et al.*, 2007). Kumari *et al.* (2007) computed average solar dimming across India throughout the winter, premonsoon, and monsoon seasons, finding that the premonsoon season had the most solar dimming, followed by winter and monsoon seasons. The presence of reflective aerosols such as sulfates, nitrates, and organics, the presence of absorbing aerosols such as BC and dust that shield the surface from solar radiation, and aerosol-induced changes in cloud microphysical properties and associated enhancement in cloud depth and albedo all contribute to solar dimming (Lau *et al.*, 2008).

### 2.13.2. The “Elevated Heat Pump (EHP)” Hypothesis

Lau *et al.* (2006) put forward the hypothesis called Elevated Heat Pump (EHP) describing atmospheric heating due to enhanced loading of absorbing natured aerosols like dust and black carbon over northern India owing induced atmospheric feedback processes leading to enhanced monsoon rainfall and earlier onset of monsoon rain. During April and May, dust particles transported from adjacent deserts to the Asian monsoon region and get accumulate to high elevation on the southern and northern slopes of the Tibetan Plateau (TP), as dust aerosol absorbs solar radiation, the atmosphere heats up, to reinforce heating over northern India black carbon (BC) from industrial pollution over the Indo-Gangetic Plain (IGP) favours the formation of anomalous large scale circulation responses over central and northern India (Lau *et al.*, 2006). The EHP mechanisms describe how the pre-monsoon accumulation of absorbing aerosols such as dust and BC causes upper-atmosphere heating, which delays the beginning of the rainy season in northern India and the Himalayan foothills (Lau *et al.*, 2008). Meanwhile, the aerosol loading decreases in June and July owing to wash out, but the heat of condensation produced by deep convection established in May acts as a driving force to reinforce the monsoon. A recent study by Kim *et al.* (2015) came to the same conclusion that during the pre-monsoon period, low level westerlies drawn moisture from the Indian Ocean and large concentrations of aerosols from the surrounding arid regions towards northern India and along the Himalayan foothills. From a study conducted over four consecutive contrasting monsoon seasons (2001-2004), Panicker *et al.*, (2010) concluded that aerosol indirect radiative forcing can cause both positive and negative forcing, with alternate years being found to be positive (2002,2004) and negative (2001,2003), which was due to changes in circulation patterns bringing up air mass containing aerosols of different sources. Over the Indian monsoon region, Das *et al.*, (2015) calculated surface shortwave radiative forcing at aerosol hot spots to be in the range of -25 to -60 W/m<sup>2</sup>. (Li & Ramanathan, 2002; Kaufman *et al.*, 2002). Aerosol forcing has a greater impact on changing internal climate system feedbacks that modify temperature gradients between land and ocean, implying that the major cause of



monsoon circulation weakening is aerosol forcing (Bollasina *et al.*, 2011). During the period 1950-1999, changes in aerosol driven forcing influenced precipitation, causing a 10-20 day earlier onset of monsoon during the transition period and a significant drop in precipitation during the peak monsoon season (Bollasina *et al.*, 2013).

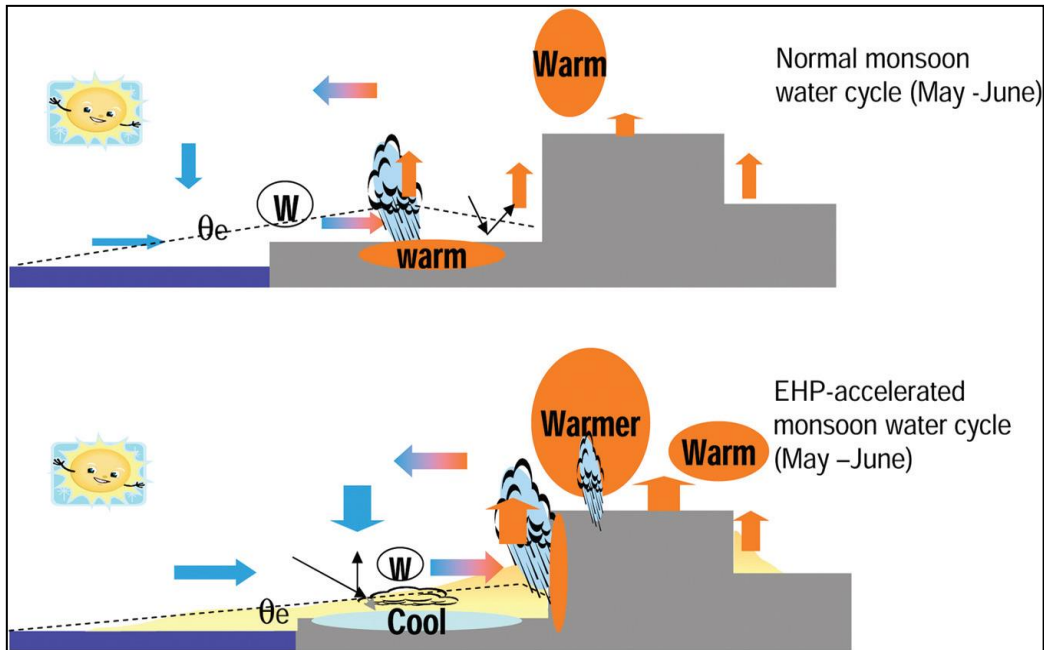


**Figure 4: schematic representation of monsoon water cycle during normal and EHP induced condition. W denotes low level westerlies and  $\theta_e$  denotes low level equivalent potential temperature. Adapted from “The Joint Aerosol–Monsoon Experiment: A New Challenge for Monsoon Climate Research” by, Lau *et al.*, 2008**

caused enhanced tropospheric heating, resulting in intense rainfall during the transition phase (May-June). They (Kim *et al.*, 2015) also attempted to correlate El-Nino Southern Oscillation (ENSO) episodes, which may serve as a major forcing agent for the EHP effect throughout the pre- and early monsoon season, as well as aerosol accumulation. According to Kim *et al.* (2015), the anomalous heating from EHP can overcome the stability effect due to the aerosol semi-direct effect.

#### 2.14. AEROSOL RADIATIVE FORCING DURING MONSOON

From a study conducted over four consecutive contrasting monsoon seasons (2001-2004), Panicker *et al.*, (2010) concluded that aerosol indirect radiative forcing can cause both positive and negative forcing, with alternate years being found to be positive (2002,2004) and negative (2001,2003), which was due to changes in circulation patterns bringing up air mass containing aerosols of different sources. Over the Indian monsoon region, Das *et al.*, (2015) calculated surface shortwave radiative forcing at aerosol hot spots to be in the range of -25 to -60 W/m<sup>2</sup>. (Li & Ramanathan, 2002; Kaufman *et al.*, 2002). Aerosol forcing has a greater impact on changing internal climate system feedbacks that modify temperature gradients between land and ocean, implying that the major cause of monsoon circulation weakening is aerosol forcing (Bollasina *et al.*, 2011). During the period 1950-1999, changes in aerosol driven forcing influenced precipitation, causing a 10-20 day earlier onset of monsoon during the transition period and a significant drop in precipitation during the peak monsoon season (Bollasina *et al.*, 2013).

#### 2.15. IMPACT OF INTERTROPICAL CONVERGENCE ZONE (ITCZ) ON AEROSOL

Several studies have found that the ITCZ has a significant impact on aerosol distribution. The relative position of the ITCZ is strongly influenced by hemispheric temperature contrasts and subsequent atmospheric restructuring, which draw the ITCZ towards the warmer hemisphere, that is, towards the northern hemisphere during boreal summer and the southern hemisphere during boreal winter (Ridley *et al.*, 2015) In turn, the position, structure, and migration of the ITCZ have a large influence on low-latitude seasonal rainfall distribution, ocean-land-atmosphere interactions, tropical ocean circulation, and a number of global climate features (Saha *et al.*, 2005). During the boreal winter, the prevailing north-easterly winds that carry polluted continental air mass downwind collide with the southward excursion of clean oceanic air mass of the ITCZ, resulting in convergence and updrafts that act as a virtual barrier shielding the

regions to its south from aerosol incursion (Saha *et al.*, 2005). Thus, years with the ITCZ located near the equator or with a slight southward extension reduce the transport of polluted air masses into the Southern Hemisphere, resulting in piling up or loading of aerosols to the north of the ITCZ, causing changes in cloud microphysical properties, whereas years with the ITCZ located south of the ITCZ exhibit significantly lower aerosol concentrations due to convective activity, mixing, and wet removal in clouds (Andronache *et al.*, 2002; Saha *et al.*, 2005).

## CHAPTER 3

### MATERIALS AND METHODS

#### 3.1. SITE DESCRIPTION

The chosen area of the study is the Indian monsoon region comprising 5<sup>0</sup>S, 50<sup>0</sup>E to 40<sup>0</sup>N, 110<sup>0</sup>E (figure 4), where the most significant monsoon activities, its origin, and propagation take place. Indian monsoon region with its diversified geographical and topographical features, dense population and urbanization, and large coastal zones, spot the region as a unique platform to execute aerosol forcing studies. The most important characteristic feature of the study area is the synoptic meteorology comprises of seasonally reversing air mass type and convective activity associated with the southwest monsoon from June to September and northeast monsoon (dry monsoon) from December to March (Ramachandran & Cherian, 2008). During the dry monsoon, the prevailing winds are generally north-easterly, which transport relatively dry air mass from the inland continental regions to the Indian Ocean, with low relative humidity and little precipitation except over the southern peninsula (Babu *et al.*, 2013) in contrast, during June to September, the steady onshore wind brings in moist laden marine air mass carrying sea salt from the Indian Ocean and mineral dust from the neighbouring desert regions over the Indian sub-continent (Ramachandran & Cherian, 2008; Babu *et al.*, 2013; Ramachandran & Kedia, 2013). October–November, and May–June months mark the transition phases of dry and wet monsoon thus carry dry continental air mass to moist marine air mass and vice versa (Babu *et al.*, 2013). The site is known to have high loading of aerosols, a variety of aerosol sources, a wide spectrum in size and distribution, and regional scale variations in its properties result in temperature anomaly, subsequently leading to strong thermodynamic effects. Because the region experiences tropical and subtropical climatic conditions, which result in significant temperature changes, rainfall, and relative humidity, there are considerable variations in aerosol properties on spatial and temporal scales in the research area (Ramachandran & Cherian, 2008). The

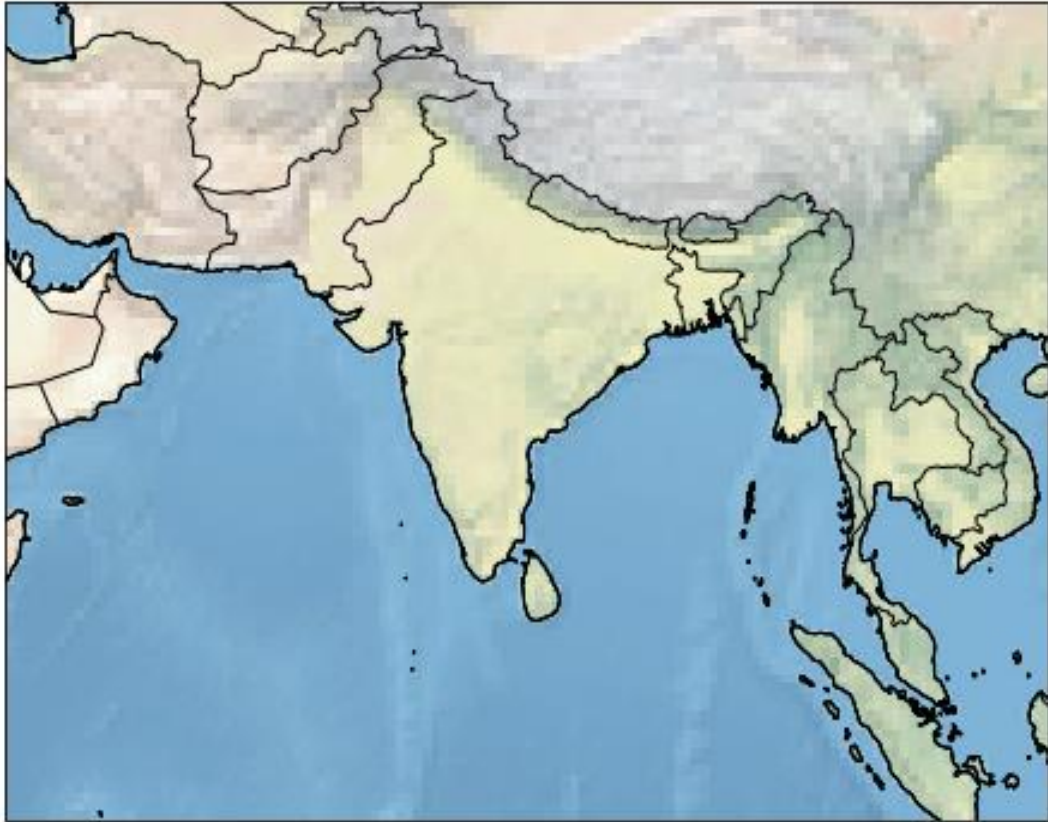


**Figure 5: Schematic representation of spatial coverage of study area comprising 5°S, 50°E to 40°N, 110°E.**

Indian subcontinent is considered as an aerosol source region, with emissions from a mix of rural and urban (74 % and 26 %, respectively) populations releasing particulate matter from biofuels such as fuelwood, dung cake crop waste, and fossil fuel emissions such as coal, petrol, and diesel oil (Ramachandran & Cherian, 2008). The India monsoon region has a variety of aerosol emission sources, and the aerosol burden over India is approximately three times higher than the global mean values due to the abundance of mineral dust, particularly during the pre-monsoon and monsoon seasons (Pandey *et al.*, 2017). Aerosol loading is generally very high over the Indian monsoon region, and the region is also characterized by substantial moisture influx due to monsoon circulation (Sarangi *et al.*, 2017), therefore our study area with heavy aerosol burden and ample moisture makes it an ideal region to study aerosol–rainfall connections.

## 3.2. DATA SETS

### 3.2.1. Aerosol optical depth: MODIS Terra & Aqua

#### *MODIS dataset*

The Moderate Resolution Imaging Spectroradiometer (MODIS) instrument, which operates on both the Terra and Aqua spacecraft, provides standard data packages. Both the Terra and Aqua satellite instruments capture the same area on Earth every 1-2 days, but their orbital times differ by about 3 hours: the Terra satellite orbits in the morning at 10:30 a.m. local time in the north to south direction, while the Aqua satellite orbits in the afternoon at 13:30 a.m. local time in the south to north direction (Verma *et al.*, 2019). The MODIS Aerosol Product can be utilized to measure the optical thickness of ambient aerosol over the oceans and continents around the world. For a long time, MODIS has provided a long-term and continuous monitoring of different aerosol optical properties, such as optical depth, types of aerosols, and aerosol size-distribution, allowing us to better understand complex atmospheric processes and varying climate dynamics over land and oceans, as well as validating and developing new models to predict climate (Verma *et al.*, 2019). The instrument has 36 spectral bands, with 19 used for land, cloud, and aerosol properties, ocean colour, atmospheric water vapour, and biogeochemistry, and the rest for surface, cloud, atmospheric temperature, atmospheric altitude, and cloud water vapour (Verma *et al.*, 2019). Aerosols that are “fine” (anthropogenic/pollution) and “course” (natural particles; e.g., dust) are also produced. There are two MODIS Aerosol data product files: MOD04 L2, which includes information from the Terra platform, and MYD04 L2, which collects information from the Aqua platform. The MOD04 L2 product offers global AOD derived from dark target (DT) and deep blue (DB) algorithms. The DT method is utilised in the water and on dark land surfaces, while the DB algorithm is performed on brighter surfaces. Many studies have used the MODIS recovered AOD to explore the variability of aerosol features at global and regional scales, including India, where an overestimation is detected in comparison to AERONET (Das *et al.*, 2015). For present study we utilize monthly averaged

MODIS derived Combined Dark Target and Deep Blue AOD at 0.55 micron for land and ocean with  $1^0 \times 1^0$  spatial resolution to analyze the aerosol concentration over the study area. This combined AOD data product is used to provide improved data coverage over both dark and bright land surfaces.

### ***Aerosol optical depth (AOD)***

Aerosol optical depth (AOD) or aerosol optical thickness (AOT) is a dimensionless quantity that measures the extinction caused by radiation interactions with aerosol particles in the atmosphere, primarily due to scattering and absorption processes, and is used to calculate aerosol column concentration. The AOD ( $\tau$ ) is defined as the integrated extinction coefficient of radiation over a vertical column of unit cross section, and it can be used as a proxy for aerosol concentration or load in a given area. AOD is a turbidity measure associated with aerosol concentrations in the atmosphere, which cause attenuation of incoming short wave radiation (AL-Taie *et al.*, 2020). Aerosol optical thickness (AOT) is the most basic and comprehensive parameter for remotely assessing the aerosol burden in the atmosphere (Holben *et al.*, 2001), as it determines the optical properties of aerosols, which is the degree to which aerosols prevent light transmission in the atmosphere through scattering or absorption (Verma *et al.*, 2019). The wavelength dependence of AOD depends on the aerosol type, that is, the physicochemical characteristics of the particles (Holben *et al.*, 2001), and measuring AOT at different spectral wavelengths (mostly visible range) helps in deriving information on the optical properties and understanding their impact on radiation balance (Verma *et al.*, 2019).. The attenuation of solar radiation passing through the atmosphere is given by the Bouguer–Beer–Lambert law also known as the Beer-Lambert Law.

### ***Beer-Lambert law***

The Beer-Lambert law relates the attenuation of light to the properties of the material in the atmosphere through which the light is travelling. Transmission of light through a volume containing aerosols can be describes using this law. The law states that there is a logarithmic dependence between the transmission (or

transmissivity),  $t$ , of light through a substance and the product of the absorption coefficient ( $\beta$ ) and the distance the light travels through the material, or the path length ( $d$ ). The equation for Beer-Lambert's law is given as:

$$t = \frac{I}{I_0} = e^{-\beta d} \quad (\text{Equation 2})$$

### 3.2.2. UV aerosol index: TOMS & OMI

TOMS (Total Ozone Mapping Spectrometer) instruments have provided valuable global data on the long-range distribution of absorbing aerosols. The TOMS ozone retrieval technique calculates an absorbing Aerosol Index (AI), which is a qualitative index of the presence of UV-absorbing aerosols such as mineral dust and smoke. The Ozone Monitoring Device (OMI) is now maintaining the long-term data record of aerosol information from the TOMS instrument. The OMI devices are the successors to the TOMS instruments, and they are targeted to monitoring ozone, air quality, and climate on the planet (Buchard *et al.*, 2015). OMI is a nadir-viewing, wide-field-imaging UV and visible spectrometer designed to monitor ozone and other atmospheric species, particularly aerosols and particles in the atmosphere, as well as to categorise aerosol types and measure cloud pressure and coverage (Verma *et al.*, 2019). It detects solar light scattered by the atmosphere in the wavelength range of 270–500 nm.

#### ***Aerosol Index (AI)***

The Aerosol Index (AI) is a qualitative index that indicates the existence of absorbing aerosols such as desert dust, biomass burning, and volcanic ash plumes (Ahmad *et al.*, 2006; Manoj *et al.*, 2011). The AI is positive for most absorbing aerosols, but negative for non-absorbing aerosols, and near zero values indicate the presence of cloud (Ahmad *et al.*, 2006). It distinguishes absorbing from non-absorbing aerosols because it provides a measure of absorption of Ultra Violet (UV) radiation by smoke and desert dust (Ahmad *et al.*, 2006). The size of AI is mostly determined by aerosol parameters such as total optical depth, single scattering albedo, particle size distribution, and altitude (Manoj *et al.*, 2011). The AI is based on wavelength-dependent variations in Rayleigh scattering in the UV



spectral band, where ozone absorption is quite low. The TOMS absorbing aerosol index (AI) is defined as the difference between the measured (aerosol effects included) spectral contrast of the 360 and 331 nm wavelength radiances and the contrast calculated from the radiative transfer theory for a pure molecular (Rayleigh particles) atmosphere or a Rayleigh atmosphere containing only permanent atmospheric gases that scatter light by Rayleigh scattering. Using the Earth Probe TOMS and Aura OMI algorithms, AI is quantitatively defined as:

$$AI = 100 \log_{10} \left[ \left( \frac{I_{360}}{I_{331}} \right)_{meas} \right] \log_{10} \left[ \left( \frac{I_{360}}{I_{331}} \right)_{calc} \right] \quad (\text{Equation 3})$$

Where  $I_{meas}$  is the measured backscatter radiance and  $I_{calc}$  is the estimated radiance for a pure Rayleigh atmosphere. Since  $I_{360}$  calc calculation uses reflectivity derived from the 331 nm measurements, the Aerosol Index definition essentially simplifies to (Ahmad *et al.*, 2006):

$$AI = 100 \left[ \log_{10} \left( \frac{I_{360\_meas}}{I_{360\_calc}} \right) \right] \quad (\text{Equation 4})$$

The OMI derived UV-Aerosol index (OMI-AI) was used in this study, which is based on a spectral contrast approach in a UV range where ozone absorption is very low. Absorbing aerosols like desert dust, smoke, BC, volcanic ash, mineral dust coated with black carbon etc. decrease the spectral contrast yielding positive values of AI. UV-AI data is a measure of how much the wavelength dependence of backscattered UV radiation from an atmosphere containing aerosols differs from that of a pure molecular atmosphere (Buchard *et al.*, 2015). We use OMAERUV gridded data product with  $1^0 \times 1^0$  spatial resolution, which is based on the enhanced TOMS version-8 algorithm that essentially uses the ultraviolet radiance data.

### 3.2.3. Aerosol extinction AOT: MERRA-2

The Goddard Earth Observing System Model, Version 5 (GEOS-5) and its Atmospheric Data Assimilation System (ADAS), version 5.12.4, are used in the MERRA-2 (Modern-Era Retrospective Analysis for Research and Applications, version-2) NASA atmospheric reanalysis for the satellite era. The MERRA

project examines historical climate assessments for a variety of weather and climate time scales. MERRA-2 is the most recent long-term global reanalysis, and it began as a bridge between the MERRA data's ageing and the next generation of Earth system analysis that would be used in future coupled reanalyses. MERRA-2 simulates natural and anthropogenic aerosols and offers data with a spatial resolution of  $0.5^\circ \times 0.625^\circ$  for the period 1 January 1980 to the present. The MERRA-2 aerosol reanalysis is a ground-breaking technique for examining air quality issues, notable for its global coverage and differentiation of aerosol speciation reported as aerosol optical depth (AOD). For near-real-time climate analysis, MERRA-2 was created to replace the original MERRA reanalysis by using current breakthroughs in modelling and data assimilation. MERRA-2 simulates natural and anthropogenic aerosols, including the sources, sinks, and chemistry of mixed aerosol tracers, as well as space-based aerosol measurements and their interactions with other physical processes in the climate system (Rizza *et al.*, 2019). MERRA-2 also makes major contributions to Earth system reanalysis and meteorological assimilation improvements.

We used extinction aerosol optical thickness (AOT) of major natural aerosol species like desert (mineral) dust and sea salt, as well as anthropogenic aerosols like sulfate ( $\text{SO}_4$ ), organic carbon (OC), and black carbon (BC) to analyse the contribution of each species during the transition phase in the Indian monsoon region (Bellouin & Haywood, 2015).

#### **3.2.4. Low level westerlies: ERA5**

We extract the u and v components of wind at 850hPa over the Indian monsoon region using the daily average ERA5 global atmospheric reanalysis dataset. The u component of the wind is the eastward component of the wind, signifying the horizontal speed of air travelling eastward. The v component of the wind is the northward component, indicating the horizontal speed of air travelling northward. Both factors (u and v) can be combined together to get the speed and direction of the resulting horizontal wind. ERA5 is the fifth generation ECMWF (European Centre for Medium-Range Weather Forecasts) reanalysis for the past 4

to 7 decades of global climate and weather. Reanalysis combines model data with observations from around the world using physics laws to create a globally complete and consistent dataset. ERA5 provides hourly estimates for a wide range of atmospheric, ocean-wave, and land-surface variables. The ERA5 hourly gridded data on pressure levels cover the period 1979 to the present and include 37 pressure levels with a vertical coverage of 1000 hPa to 1 hPa and a horizontal resolution of  $0.25^\circ \times 0.25^\circ$ .

### **3.2.5. Rainfall: IMD gridded rainfall**

India Meteorological Department (IMD) has released a new daily gridded rainfall data set of 120 years (1901-2020). This data package is a daily gridded rainfall data measured in millimetres (mm) with a very high spatial resolution ( $0.25 \times 0.25$  degree). In order to compare the rate of precipitation over IGP (heavy loading of aerosol) and Kerala (lower aerosol concentration) we collect daily gridded rainfall dataset for a period of 4 years (2017-2020)

### **3.2.6. Radiative fluxes: CERES-SYN1deg Ed4A**

The Earth Observing System (EOS) project Clouds and the Earth's Radiant Energy System (CERES) uses broadband channels to provide satellite-based radiometric measurements and observations of the earth radiation budget (ERB) and clouds. The CERES instruments use three broadband channels to provide radiometric measurements of the Earth's atmosphere by combining measurements from CERES instruments on several satellites with data from many other instruments to create a comprehensive set of ERB data products for climate, weather, and applied science research. There are now six operational CERES flight models (FM1, FM2, FM3, FM4, FM5 & FM6). FM1, FM2, CERES Scanner, and Moderate-Resolution Imaging Spectroradiometer (MODIS) on Terra; FM3, FM4, CERES Scanner, and MODIS on Aqua; FM5 on board the Suomi National Polar-orbiting Partnership (NPP) satellite; and the final CERES instrument FM6 on board the National Oceanic and Atmospheric Administration's (NOAA) Joint Polar Satellite System 1 (JPSS-1) satellite. To show the aerosol-induced variations in radiative forcing, CERES derived shortwave and longwave

fluxes under two alternative scenarios, namely all sky with aerosols and all sky without aerosols were considered.

Data	Data set	Period	Resolution	Download link
Aerosol Optical Depth (AOD) @ 550nm	MODIS Terra & Aqua	2017-2020	1 <sup>0</sup> x 1 <sup>0</sup>	<a href="https://giovanni.gsfc.nasa.gov/giovanni/">https://giovanni.gsfc.nasa.gov/giovanni/</a>
Wind @ 850hPa	ERA5	2017-2020	0.25 <sup>0</sup> x 0.25 <sup>0</sup>	<a href="https://cds.climate.copernicus.eu/cdsapp#!/dataset/reanalysis-era5-pressure-levels?tab=form">https://cds.climate.copernicus.eu/cdsapp#!/dataset/reanalysis-era5-pressure-levels?tab=form</a>
Aerosol index (AI)	TOMS & OMI	2017-2020	1 <sup>0</sup> x 1 <sup>0</sup>	<a href="https://giovanni.gsfc.nasa.gov/giovanni/">https://giovanni.gsfc.nasa.gov/giovanni/</a>
Aerosol extinction AOT	MERRA-2	2017-2020	1 <sup>0</sup> x 1 <sup>0</sup>	<a href="https://giovanni.gsfc.nasa.gov/giovanni/">https://giovanni.gsfc.nasa.gov/giovanni/</a>
Radiative flux	CERES-SYN1deg Ed4A	2017-2020	1 <sup>0</sup> x 1 <sup>0</sup>	<a href="https://ceres.larc.nasa.gov/data/">https://ceres.larc.nasa.gov/data/</a>
Rainfall	IMD	2017-2020	0.25 <sup>0</sup> x 0.25 <sup>0</sup>	<a href="https://www.imdpune.gov.in/Clim_Pred_LRF_New/Grided_Data_Download.html">https://www.imdpune.gov.in/Clim_Pred_LRF_New/Grided_Data_Download.html</a>

**Table 1: Satellite derived daily and monthly dataset used in this study**

### 3.3. DATA ANALYSIS

The spatial distribution of aerosols (both natural & anthropogenic) must be documented in order to study the sensitivity of aerosol loading across the Indian monsoon region. Choudhury *et al.*, 2020 found a positive and significant relationship between AOD at 550nm and aerosol-induced radiative forcing, with a high correlation coefficient at the surface and a moderate correlation coefficient at the top of the atmosphere. To examine the spatial distribution of aerosol burden we make use of AOD dataset @550nm derived from MODIS instrument on board Terra satellite to analyze the temporary average (2017-2020) of aerosol burden over the Indian monsoon region. As the study area includes a variety of environments such as coastal, marine, arid, continental, and urban, each of which represents distinct aerosol emission sources that influence aerosol speciation, distribution, and removal mechanisms (Sajani et al., 2021). It is also essential to distinguish the contribution of each major aerosol species (dust,BC,sulfate,sea salt,OC).

In addition, we investigate the considerable strength and pattern of low-level westerlies, which play an important role in the transport and loading of aerosol particles. We employ U & V components of wind data at 850 hPa generated from ECMWF-Era5 reanalysis data during the transition phase of south west monsoon by dividing the entire period from the second half of May to the first half of June into six sub-periods (pentads) for a systematic understanding of low level westerlies, which is illustrated in the table 2.

Sub-periods	Days
1	May 17-May 21
2	May 18-May 26
3	May 27-May 31
4	Jun1-jun5
5	Jun6-jun10
6	Jun11-jun15

Table 2: categorization of transition period into sub-periods

In the study, an aerosol index data derived from OMI was employed to recognize the source region and transit of absorbing aerosol; in fact, the index captures dust, smoke, and volcanic ash. AI data over the whole monsoon period is used to compare the transport of absorbing aerosols throughout the transition, advancing, and peak phases of the south west monsoon.

The radiative impact of aerosols on atmospheric circulation over India during the summer monsoon season was investigated in this study. To compute aerosol radiative forcing in the atmosphere we use CERES (Clouds and the Earth's Radiant Energy System) daily data of radiation fluxes with  $1^0 \times 1^0$  spatial resolution. To investigate the radiative impact of aerosols during the transition phase over the study period (2017-2020), we chose two regions, one with the highest aerosol loading and the other with the lowest aerosol level based on aerosol optical depth analysis. The selected regions are Indo-Gangetic Plain (IGP) region ( $75^0$ - $92^0$ E,  $22^0$ - $22^0$ N) is characterized by high aerosol burden and the equatorial Indian Ocean (EIO) region ( $50^0$ - $95^0$ E,  $5^0$ S- $7^0$ N) that has the lowest aerosol concentration. The difference in net radiative fluxes at the surface (SRF) and at the top of the atmosphere (TOA) with and without aerosols is characterized as direct aerosol radiative forcing (ARF). The two principal radiative fluxes recognized are shortwave radiation(S) and long wave radiation (L). Radiative forcing at the surface and TOA is defined as the perturbation in the surface reaching solar intensity and up-scattered solar radiation flux under all sky with aerosols and all sky without aerosols conditions are considered. The net flux ( $R_{net}$ ) can be calculated as:

$$R_{net} = [S_{(down)} - S_{(up)}] + [L_{(down)} - L_{(up)}] \quad (\text{Equation 5})$$

The difference in radiation components between all sky (aerosols present) and all sky no aerosol (low or no aerosols clouds) is used to determine aerosol forcing (ARF) at the surface and TOA.

$$ARF_{(SRF)} = [F_{(all\ sky)} - F_{(noaero)}]_{(SRF)} \quad (\text{Equation 6})$$

$$ARF_{(TOA)} = [F_{(all\ sky)} - F_{(noaero)}]_{(TOA)} \quad (\text{Equation 7})$$

Where,  $ARF_{(SRF)}$  denotes aerosol radiative forcing at the surface,  $ARF_{(TOA)}$  represents Aerosol radiative forcing at top of the atmosphere and  $F$  denotes net flux during all sky and all sky with no aerosol conditions

The atmospheric forcing explains the amount of energy trapped by the aerosols. Aerosol radiative forcing (ARF) at the atmosphere is calculated by considering the difference between net radiative forcing at the TOA and surface

$$ARF_{(ATM)} = ARF_{(TOA)} - ARF_{(SRF)} \quad (\text{Equation 8})$$

The rate of heating caused by aerosols is a key component in determining climatic patterns (Nair *et al.*, 2017). The Santa Barbara Discrete Ordinate Radiative Transfer (SBDART) model, which is a FORTRAN computer code designed to simulate radiative fluxes at the top of the atmosphere and surface, can be used to estimate the vertical profiles of aerosol heating rate fluxes at various height levels using the following equation(Nair *et al.*, 2017; Sivan & Manoj, 2019):

$$\frac{\partial T}{\partial t} = \left( \frac{g}{C_p} \right) \left( \frac{ARF_{ATM}}{\Delta P} \right) \quad (\text{Equation 9})$$

Where  $\partial T/\partial t$  is aerosol heating rate,  $g$  is the gravitational acceleration,  $C_p$  is the specific heat at constant pressure and denotes the vertical extend of the atmosphere which is influenced by the aerosol radiative forcing.

Intra-seasonal and inter-annual variability in the monsoon circulation and rainfall over India could be caused by aerosols (Manoj *et al.*, 2011; Sajani *et al.*, 2021). We have examined co-variability of aerosol and monsoon precipitation on a regional basis. The states of Kerala and IGP were chosen to investigate the regional effects of aerosol-monsoon interactions on monsoon variability. Aerosol loading and rainfall distribution in South Asian regions exhibit considerable spatial gradients linked with topographic differences (Dipu *et al.*, 2013), implying that regional-based investigation is required for detecting aerosol-precipitation interactions. Therefore, impact of aerosol-monsoon interactions on monsoon variability was chosen to be studied in Kerala and the IGP. Kerala is the region where the monsoon begins and is distinguished by a low aerosol burden due to the

washout effect, whereas the IGB is distinguished by a rich supply of aerosol and is marked as the monsoon's northern limit.

### ***Indo Gangetic Plain (IGP)***

Satellite derived observational evidence from the Terra/Aqua MODIS enhanced AOD @ 550nm revealed that the aerosol burden over IGP was greater than the overall study area's mean value of AOD. The Indo-Gangetic Plain (IGP) is regarded as a global hotspot of elevated aerosol loading, or a region of aerosol pool that has experienced aerosol enhancements and persistence due to seasonality and topography (Gautam *et al.*, 2011; Manoj *et al.*, 2011; Babu *et al.*, 2013; Kumar *et al.*, 2018). Because of growing population and economic growth, the IGP region is one of the most polluted in the world. It is located in northern India and is surrounded by a unique topography that includes the Himalayan foothills to the north and hills to the south. The presence of absorbing aerosols such as dust and BC was found to have a single scattering albedo (SSA) greater than 0.9, implying that these coarse mode particles, which influence longer wavelengths, are short-lived and thus produce effects that are more local in nature (Gautam *et al.*, 2011).

### ***Kerala***

Kerala's AOD was found to be moderate to low, and it is the region where the monsoon season begins over the Kerala coast, which is linked to numerous changes in large-scale dynamical parameters as well as local moisture parameters (Mehta, 2015). Although the concentration of aerosols in south India is lower than in north India, the seas that surround the region have a significant impact on aerosol loading because they are sources of marine aerosols such as sea salt and sulphates, which can cause aerosol exchange between the marine and land environments (Sivaprasad & Babu, 2016). As a result, analysing the co-variability between aerosols and monsoon precipitation is critical for obtaining precise information on the regional impact of aerosols.



## CHAPTER 4

### RESULTS

#### 4.1. SPATIAL DISTRIBUTION OF AEROSOL CONCENTRATION

AOD derived from the Moderate Resolution Imaging Spectroradiometer (MODIS) instrument on board Terra satellite is used to analyze the spatial average of aerosol burden over the Indian monsoon region over the study period (2017-2020) which is illustrated in the figure 6. As the atmospheric aerosol particles

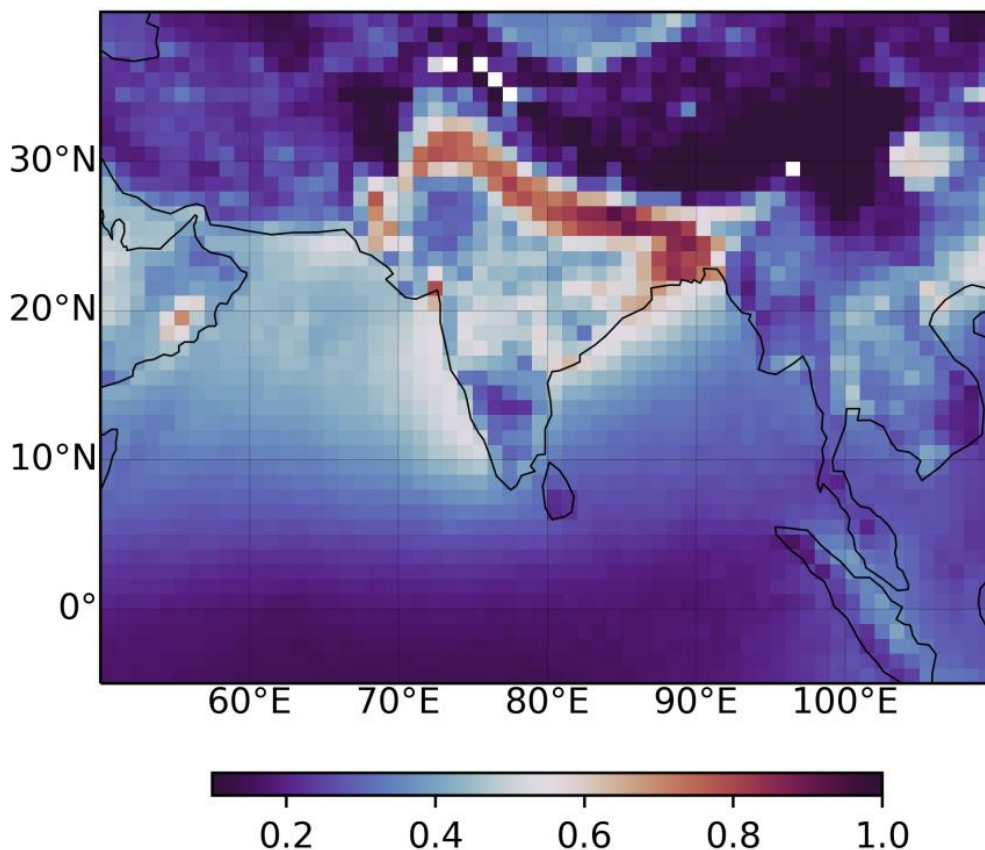


Figure 6: Temporal average of AOD over Indian monsoon region during the period of study

display a high temporal and spatial variability depending upon the source and ambient surrounding atmospheric conditions (Babu *et al.*, 2013), there is a possibility for fast, relatively regionalized, changes in forcing and temperature response. IGP and Thar Desert are the two primary aerosol hotspots in the Indian subcontinent, with AOD levels ranging from 0.6 to 0.8. A continuous broad band

of high aerosol concentration may be seen over northern India, ranging from the Thar Desert in the northwest through the Himalayan foothills to the IGP in the northeast. In comparison to the IGP and the Himalayan foothills, the Tibetan plateau exhibits considerably lower aerosol deposition. Aerosol concentration was most pronounced over the northern Arabian Sea compared to the southern Arabian Sea and Bay of Bengal. During the study period, the temporary average of aerosol load remained at a peak range (0.6-0.8) primarily over the northern India including Great Indian Desert and IGP. In comparison to northern India, the aerosol levels in the southern Indian peninsular region were significantly lower. In comparison to the southern Indian peninsula and northeastern India, the average aerosol burden in central India is quite high, with AOD values ranging from 0.4 to 0.6, indicating a strong aerosol loading. Taking into account all individual maxima and minima, the spatial average of AOD over the entire study area was determined to be 0.3. The highest aerosol loading regions, such as IGP and the Indian arid region had AOD values that were twice as high as the overall spatial average.

#### 4.1.1. **Spatial distribution of aerosols during summer monsoon**

The seasonal mean of aerosol concentration over the Indian monsoon region was found to be higher than the annual mean during the summer southwest monsoon period (June to September), indicating higher loading over aerosol during summer (figure 7). During the wet monsoon (south west monsoon), heavy aerosol loading (AOD > 0.6) was observed over the northern Arabian Sea, particularly above 15<sup>0</sup>N, compared to the rest of the northern Indian Ocean. During the wet monsoon, there is a marked increase in aerosol accumulation over the Indian subcontinent, which is more pronounced in northern India than in southern India and in north eastern India than in northwestern India. We use the classification provided by AL-Taie *et al.* (2020) in table 3 to analyze the aerosol type-wise distribution based on AOD. Using the table, it can be inferred that a variety of aerosol species were found across the study area, with a significant contribution of mineral dust from dust and also aerosols emitted from biomass burning over central and northern India. The highest aerosol loading regions, such as the IGP

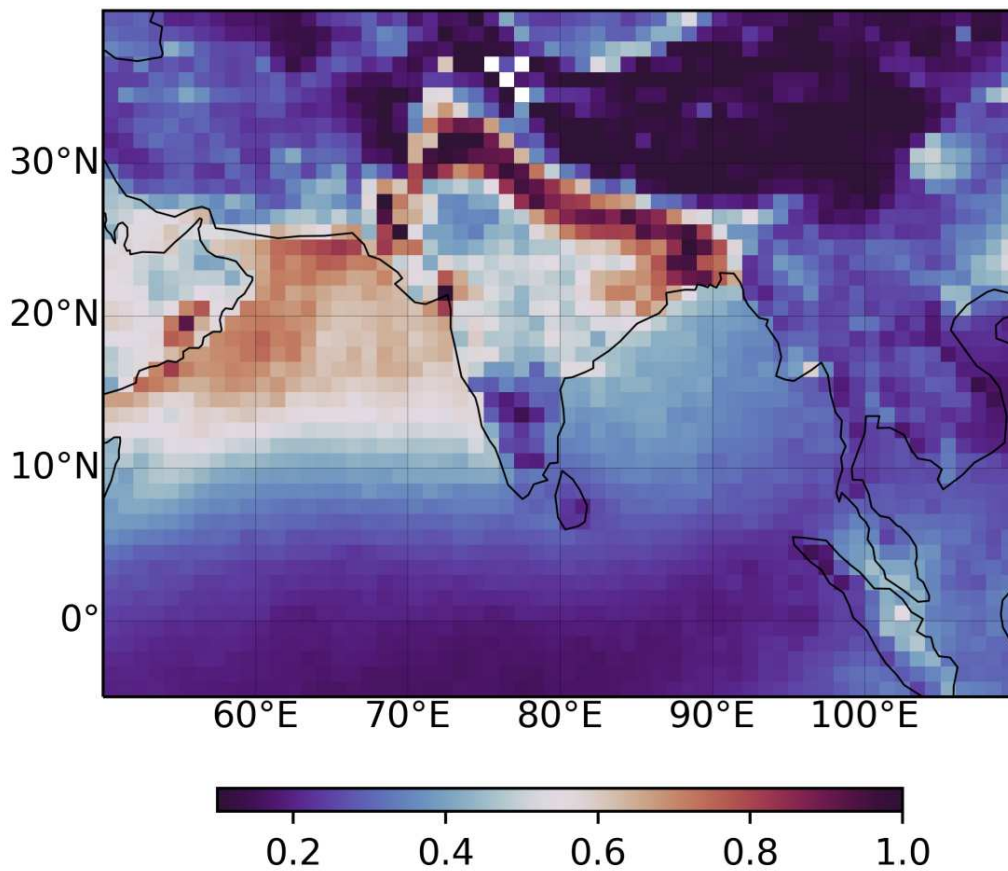


Figure 7: Temporal average of AOD during the south west monsoon over the Indian monsoon region during the period of study.

Aerosol type	Aerosol optical depth (AOD)
Maritime	< 0.3
Dust	> 0.4
Urban	0.2-0.4
Desert dust	> 0.45
Biomass burning	>0.7

Table 3: Classification of aerosol types based on AOD.

and the Indian arid region had AOD values that were twice as high as the overall spatial average, indicating the importance of paying more attention to this area in order to make an accurate assessment of regional aerosol impact on radiative transfer. Aerosols of the maritime and urban types were more prevalent in

southern India. The intraseasonal variation in the spatial distribution of aerosols during the south west monsoon must be analyzed to gain a better understanding of the phenomenon, which is depicted in Figure 8.

#### 4.1.2. **Spatial distribution during sub phases of the summer monsoon**

Aerosol loading also showed intraseasonal variability in their transport and accumulation, which is illustrated in figure 8. A slight increase in aerosol concentrations over the Indian monsoon region is observed during the transition phase of the south west monsoon, compared to the temporary average of aerosol concentrations over the entire south west monsoon period, as shown in figure 8a. During these phase a notable increase in aerosols can be found over both eastern and western peninsular coast of India with AOD concentration raging from 0.5 to 0.7. Aerosol load was found to be higher over the IGP, with average values ranging from 0.6 to 0.7 and heavy accumulation over the eastern IGP (0.9-0.1) compared to the western IGB.

Figure 8b shows that the spatial extent of heavy aerosol loading increased during the advancing phase, with a significant band of heavy aerosol ( $>0.7$ ) extending from the northwestern arid region to the eastern end of the IGP. Aerosol concentrations were higher (0.6-0.8) over the northern Arabian Sea and associated western peninsular coast of India during this sub phase (advancing phase), indicating the presence of dust loading from the western arid region, while aerosol concentrations were lower over the Bay of Bengal region and associated eastern peninsular coast of India compared to the transition phase. The average aerosol concentration over South India is reduced ( $<0.4$ ) compared to the transition phase (0.4-0.5).

During the peak phase, as shown in figure 8c, the longitudinal extent of the heavier band of aerosols that formed over northern India shrank towards the northwest, resulting in a slight decrease in aerosol concentration over the north eastern IGB and an increase in aerosol burden over the northwestern arid region

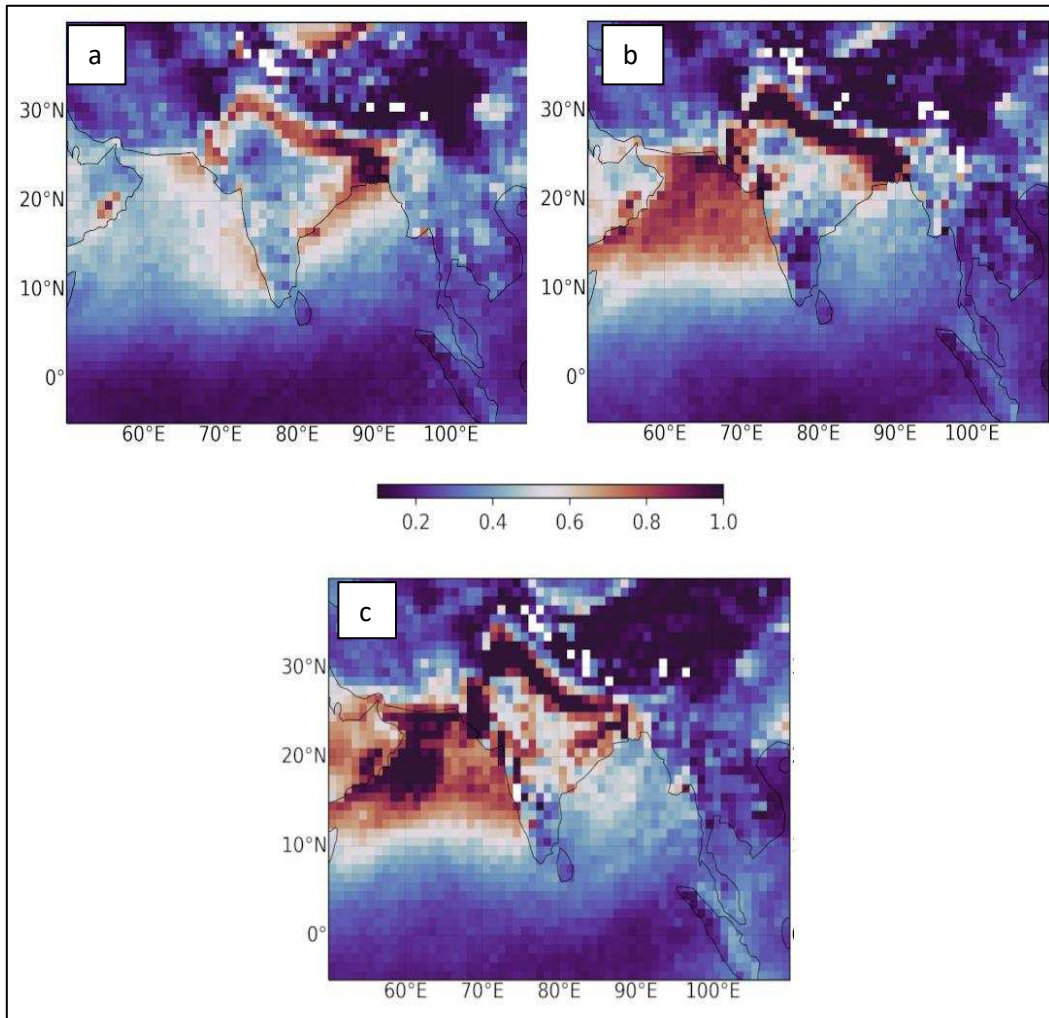


Figure 8: Intraseasonal variation of spatial distribution of aerosols during summer monsoon from 2017 to 2020. (a) Composite average of AOD during the transition phase, (b) Composite average of AOD during the advancing phase, and (c) Composite average of AOD during the peak phase.

In comparison to the previous phase, an aerosol loading was further enhanced over the northern Arabian Sea. When the total averaged aerosol concentration is calculated over the entire study area, it can be seen that the total averaged aerosol concentration increases towards the peak phase, but there exist regional variations that can be either aerosol loading or retrieval.

#### 4.2. LOW LEVEL WESTERLIES

During the wet (Southwest monsoon) and dry (Northeast monsoon) seasons, the recurrent seasonal reversal of wind systems plays a critical role in controlling

aerosol loading over the Indian subcontinent. In the present study we had examined wind systems at 850 hPa to analyze the pattern and strength of low level westerlies during the transition phase of wet monsoon as shown in the figure 9. The pentads (sub-periods) clearly demonstrate that the northward moving surface easterlies (trade winds) deflected to the left in the southern hemisphere and to the right as they cross the equator. After crossing the equator, the westerlies split into two branches: the Arabian Sea branch, which hits the Indian west coast and has one weak branch that travels to northwest India, and the Bay of Bengal branch, which passes along the southern tip of the Indian Peninsula and flows to the northeastern parts of India and it has another branch that recurves westward and moves northwestward along the Gangetic plain until meet up with the weakening air from the Arabian sea branch in the Punjab. During the first sub-period, weak to moderate south westerlies were observed across the majority of the Asian monsoon zone, with the exception of the Somali coast and the south coast of Sri Lanka ( $70^{\circ}$  - $90^{\circ}$  E and  $0$ - $5^{\circ}$  N), where strong westerlies were observed, and they intensified further during the advancing sub-periods. During the third sub-period, strong south westerlies (10-15 m/s) sweep across a broad area ranging from the southeastern edge of the Arabian Sea to the Burma coast of the Bay of Bengal. The mean resultant south westerly wind intensifies considerably in the fourth sub-period, covering a broad belt stretching from the Somali coast to the Arabian Sea.

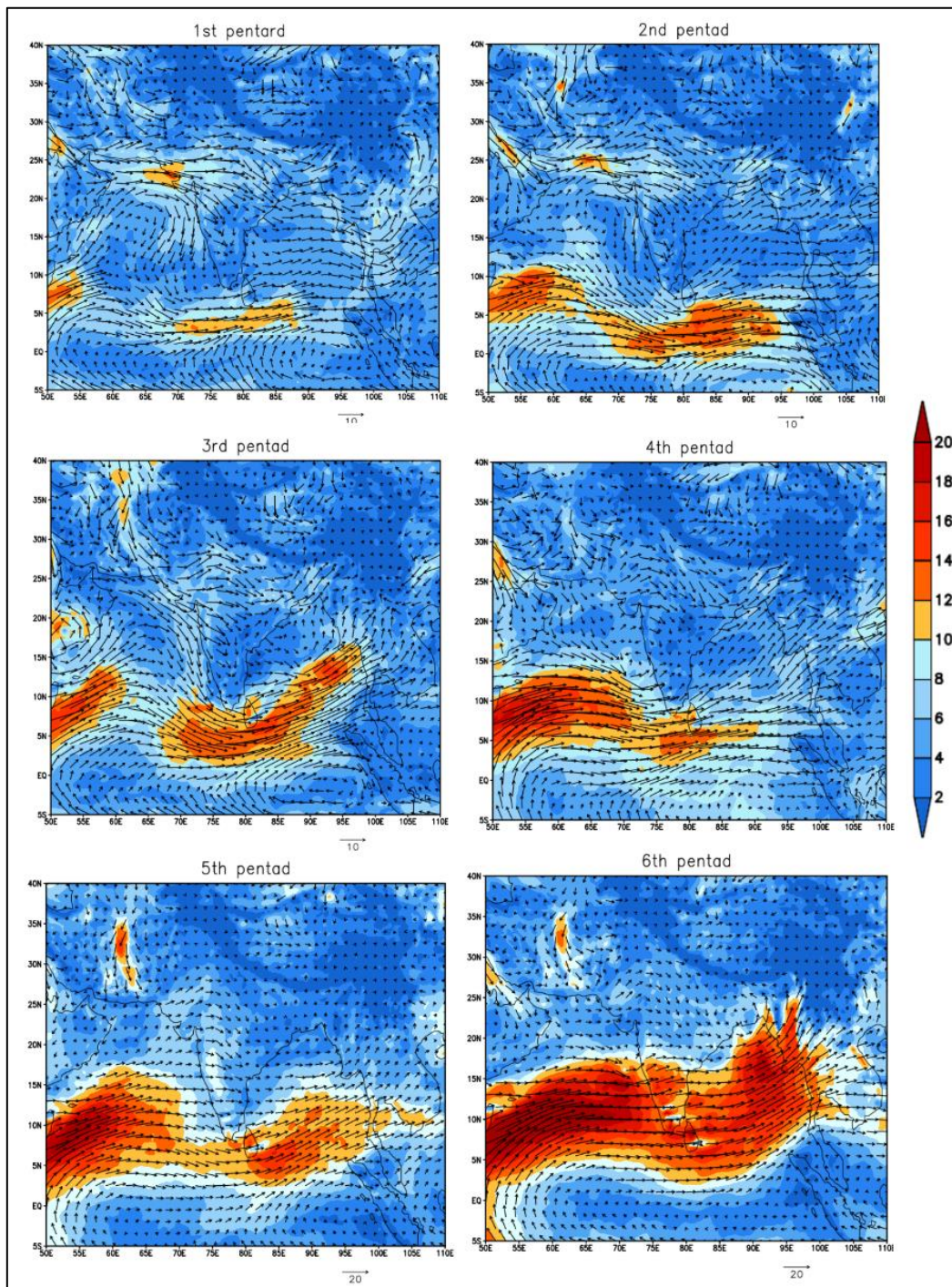


Figure 9: Mean of surface westerlies (m/s) at 850hPa during the subperiods of transition phase from 2017-2020 using ERA5 reanalysis.

intensified further during the advancing sub-periods. During the third sub-period, strong south westerlies (10-15 m/s) sweep across a broad area ranging from the southeastern edge of the Arabian Sea to the Burma coast of the Bay of Bengal.

The mean resultant south westerly wind intensifies considerably in the fourth sub-period, covering a broad belt stretching from the Somali coast to the Arabian Sea. Both the longitudinal and latitudinal extent of intense surface westerlies enhanced in the later sub-periods of 5 and 6, and more organized and strong surface westerlies were observed during these sub-periods. During the last sub-period, a well-defined continuous broad band of well-intensified south westerlies (15 - 20 m/s) were observed spreading from the Somali coast in the west Asian region to the Burma coast in the east Asia. Continental migration of surface westerlies is more pronounced during the 6<sup>th</sup> sub-period. Low-level westerly winds are prevalent over extensive zonal regions between 5°–15°N, spanning from 50°E–110°E during the monsoon transition period of May–June.

#### 4.3. AEROSOL SPECIES WISE DISTRIBUTION

We investigated the percentage distribution of aerosols throughout the transition phase during the period of study which is illustrated in the figure 10. The results show that dust, a major absorbing type of aerosol (40.7%), which was more prevalent over arid, semi-arid regions of the Indian monsoon region, contributes the most, followed by SO<sub>4</sub> (27.5 %), a scattering type of aerosol found mostly throughout the Indian subcontinent and particularly prevalent over the IGB region. Sea salt (20.4%) is the third contributor, which is predominant over the Arabian Sea and is delivered to the Indian subcontinent by low level westerlies and 3.2%, respectively), which are produced through the during the southwest monsoon. Organic carbon (OC) and black carbon (BC) aerosols (8.1% combustion of fossil fuels and biofuels, and other natural biogenic emissions, contribute the least. Al-Sahini (2018) found a similar finding in a study done in Baghdad, stating that dust type particles contributed the most (40%) to total aerosols, followed by carbonaceous (OC & BC) type aerosols (29 percent). This



suggests that dust contributes the majority of total aerosols in the atmosphere.

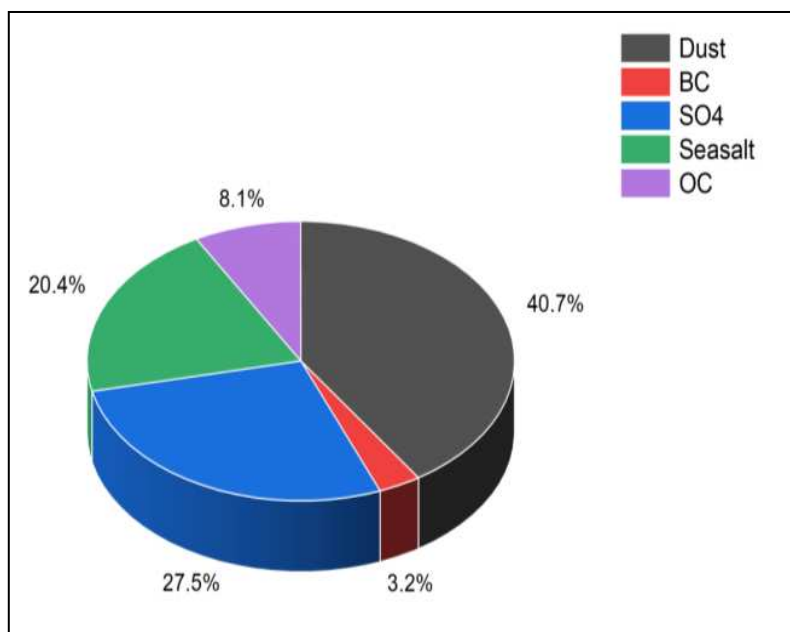


Figure 10: Aerosol species wise contribution over the Indian monsoon region over the period of study

#### 4.4. AEROSOL INDEX

AI is based on wavelength depended changes in Rayleigh scattering in the UV spectral range, where ozone absorption is extremely low, it is particularly well suited to measuring or detecting the presence of elevated layer of absorbing aerosols especially dust, black carbon and volcanic ash above high reflecting surfaces. Absorbing and non-absorbing aerosols exhibited spectral variations in backscattered radiance near the UV range; using this property, highly absorbing aerosols such as dusts can be distinguished from non-absorbing aerosols such as sulfates (Torres *et al.*, 1998). In contrast to the significant aerosol loading over the western IGP, the eastern IGP is associated with a lower average AI value, which continues to decrease in the following phases. The source regions of AI were identified to be the major

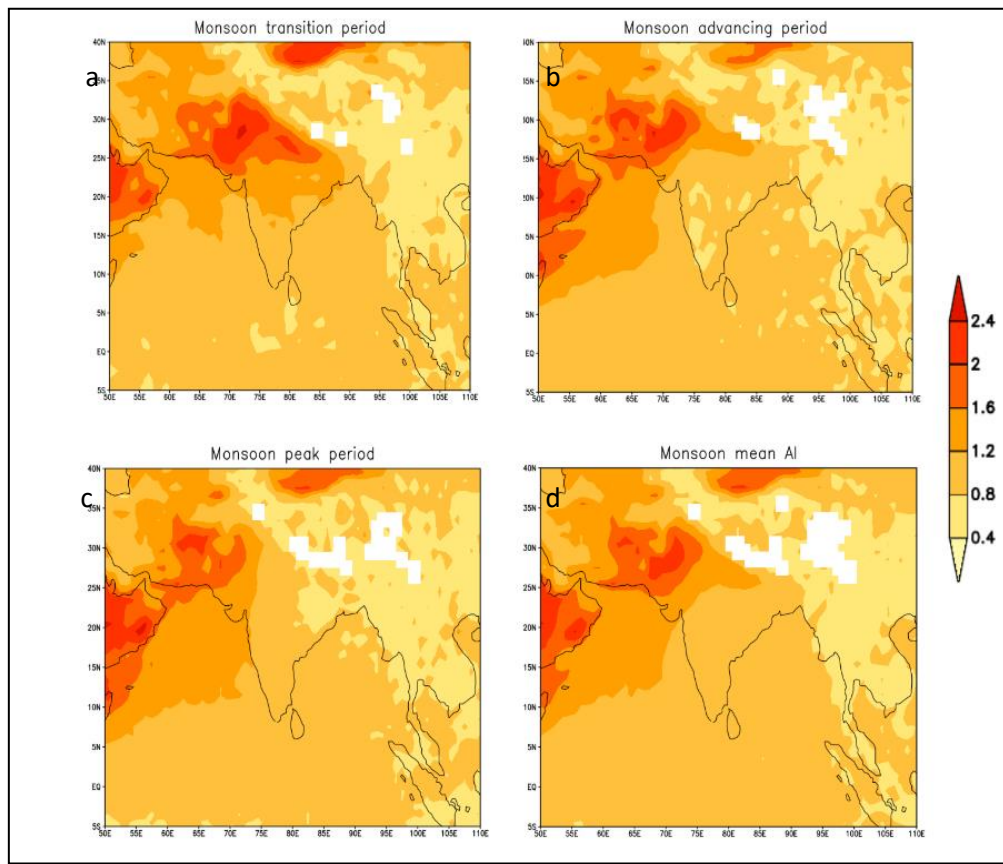


Figure 11: composite Aerosol Index during a) transition period, b)advancing period, c) peak period and the d) wet monsoon period over Indian monsoon region for a period of 2017-2020.

arid regions. Three key AI source regions were identified across the Asian monsoon region, which closely overlay significant desert and surrounding regions such as (I) Thar and Pakistan deserts, (II) Arabian deserts, and (III) Taklimakan deserts. The rectangular squares in the figure 11d of AI during monsoon represent the key source regions. Absorbing aerosols from surrounding arid regions rapidly collect considerably above the IGB region during the monsoon transition period (May 15 to June 15). During the transition period AI found to be quite high over the northern and central regions of India compared with the rest of peninsular India as shown by the figure 11a. AI was found to be fairly high in the northern and central regions of India in comparison to the rest of peninsular India during the transition phase. All India mean AI reduced during the advancing phase (June 16 to July 15) following a spike in early or transition phase and declined further in

the latter half of July (monsoon peak period). Long-range transport of dust associated with low-level westerlies from the Arabian Peninsula over the northern Arabian Sea, particularly above 10<sup>0</sup>N, leads in AI values ranging from 1.6 to 2.0. The absorbing aerosol loading over the northern Arabian Sea continues to increase in the later phases of the monsoon and achieves a high degree of spatial extend during the peak monsoon period, which can be attributed to strong monsoon wind-blown dust aerosols. However, the rest of equatorial India, including the South Arabian Sea and the Bay of Bengal, maintains AI values in the range of 1.2-1.6 during the monsoon season. During the transition, low-level westerlies transport dust particles from the Middle East and western Thar Desert to the IGP, where they build up a layer of absorbing aerosols before gradually dissipating as the monsoon moves across northern India. During the advancing and peak stages of the monsoon, absorbing aerosols are pushed and longitudinally stretched towards the northwestern region.

#### 4.5. AEROSOL RADIATIVE FORCING IN THE ATMOSPHERE

We used numerical aerosol forcing calculations, as mentioned in session 3.3, to better understand the impact of aerosol loading on regional radiation flux distribution. Radiative forcings at the top of the atmosphere (TOA) and at the surface are defined as changes in the up-scattered solar radiation flux and the surface reaching solar intensity, respectively, as a function of the AOD (Sarkar *et al.*, 2006). To investigate the regional impact of aerosols during the transition phase over the study period (2017-2020), we chose two regions, one with the highest aerosol loading and the other with the lowest aerosol level. The Indo-Gangetic Plains (IGP) region (75<sup>0</sup>-92<sup>0</sup>E, 22<sup>0</sup>-22<sup>0</sup>N ) is characterized by high aerosol transport and loading during the transition phase, while the equatorial Indian Ocean (EIO) region (50<sup>0</sup>-95<sup>0</sup>E, 5<sup>0</sup>S-7<sup>0</sup>N) has the lowest aerosol concentration. In the IGP region, the temporary average of aerosol generated surface radiative forcing increased rapidly with each phase, but the EIO region showed a very minor drop. Figure 12 clearly shows that ARF had a large intraseasonal variation during the wet monsoon. When the entire Indian monsoon

region is considered, the aerosol induced net radiative forcing in the atmosphere remains relatively constant between seasons, even though there are large spatial variations. Figure 12 clearly shows that aerosol-induced radiative forcing in the atmosphere over the IGP decreased towards the peak phase of monsoon, whereas a spike in radiative forcing was observed over the Indian monsoon region's northwestern arid region and northern Arabian Sea during the advancing phase

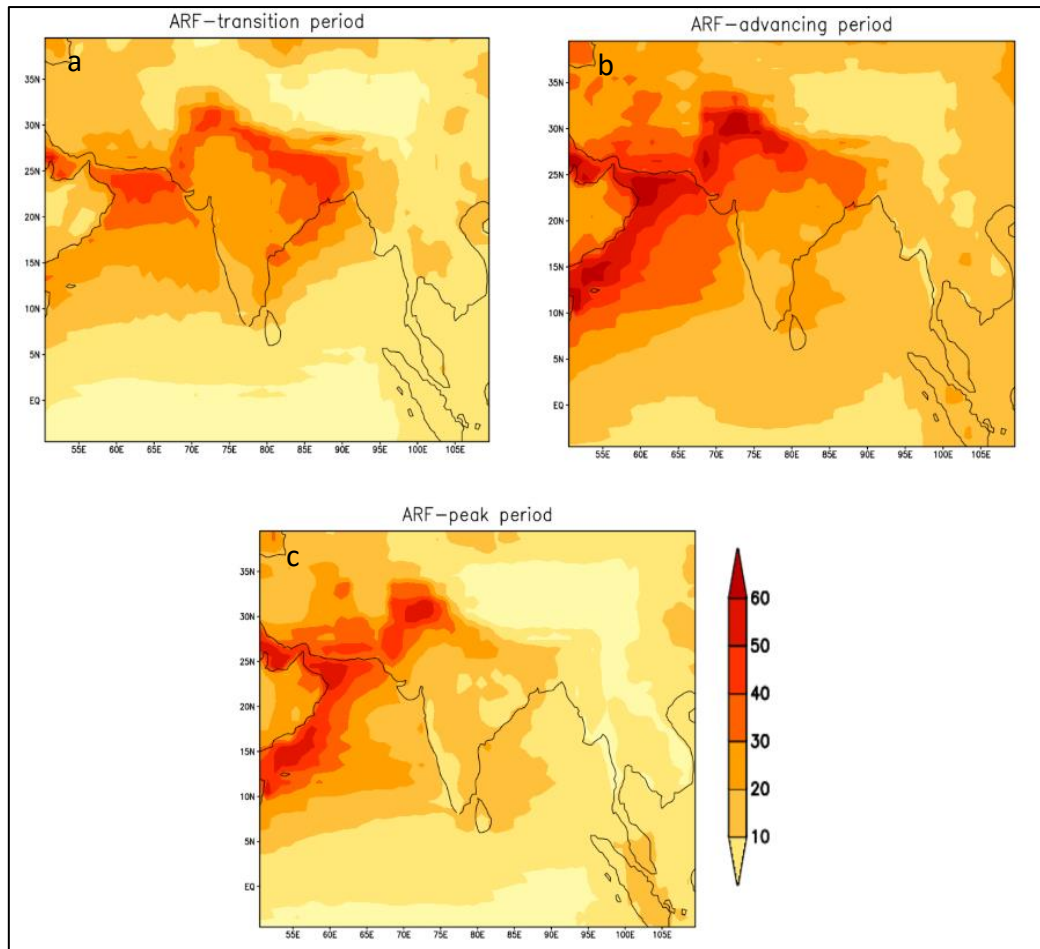


Figure 12: Composite average of intraseasonal aerosol radiative forcing over a period of 2017-2020 during, a) transition period, b) advancing period and c) peak period over a period of 2017-2020

but then showed a slight decline during the peak phase. During the phase transformations, the composite mean of ARF over TOA in the IGP region was observed to be in the range of  $5.5 \text{ W/ m}^2$  to  $9.5 \text{ W/ m}^2$ , with a slight decreasing trend, whereas in the EIO region, the composite mean of ARF over the TOA was

observed to be in the range of 3.3 W/ m<sup>2</sup> to 5.5 W/ m<sup>2</sup>, with a slight increasing trend towards the peak phase (table 4). The difference between

Year	Forcing for	Monsoon transition period (May 15- Jun15)		Monsoon advancing period (Jun 15-jul 15)		Monsoon peak period (Jul 15- Aug 15)	
		ARF_IGP (W/m2)	ARF_EIO (W/m <sup>2</sup> )	ARF_IGP (W/m2)	ARF_EIO (W/m <sup>2</sup> )	ARF_IGP (W/m2)	ARF_EIO (W/m2)
2017	ARF(TOA)	9.63	3.74	6.98	4.11	4.7	4.12
	ARF(SRF)	-31.45	-7.48	-23.1	-8.41	-17.07	-8.71
	ARF(ATM)	41.08	11.22	30.08	12.52	21.77	12.83
2018	ARF(TOA)	11.86	3.38	9	4.23	5.18	4.5
	ARF(SRF)	-41.09	-7.05	-28.3	-9.08	-19.5	-9.37
	ARF(ATM)	52.95	10.43	37.3	13.31	24.68	13.87
2019	ARF(TOA)	8.29	3.07	8.8	3.84	5.99	4.55
	ARF(SRF)	-28.4	-6.6	-27.43	-8.07	-20.05	-9.86
	ARF(ATM)	36.69	9.67	36.23	11.91	26.04	14.41
2020	ARF(TOA)	8	3.02	7.19	3.51	6.07	3.3
	ARF(SRF)	-26.9	-6.28	-22.78	-7.27	-19.08	-7.1
	ARF(ATM)	34.9	9.3	29.97	10.78	25.15	10.4

Table 4: Values for aerosol radiative forcing at the top of the atmosphere, surface and atmosphere during transition phase, advancing phase and peak phases of monsoon

the ARF at TOA and the surface yields a positive net result, implying that the aerosol radiative force has a strong warming effect in the atmosphere. Throughout the wet monsoon period, aerosol-induced radiative forcing in the atmosphere was greatest over IGB and lowest over EIO; however, the greatest difference in

atmospheric radiative forcing occurs during the transition phase. Considering the yearly variation in radiative forcing over the entire study area from 2017 to 2020, the lowest value of aerosol radiative forcing was recorded in 2020. During the transition phase over IGB, the maximum value of atmospheric forcing ( $52.95 \text{ W/ m}^2$ ) was recorded in 2018, while the least value ( $34.9 \text{ W/ m}^2$ ) was observed in 2020. Positive aerosol radiative forcing (warming impact) was recorded in the TOA over both IGP and EIO, whereas negative values (cooling impact) were reported over the surface.

One interesting observation was that atmospheric radiative forcing was estimated to be higher over the IGB region during the transition phase, but higher over the EIO region during the peak phase. It was noticed that the resultant values of atmospheric aerosol radiative forcing drops as the monsoon progresses (transition period–advancing period–peak period) Aerosol induced radiative forcing in the atmosphere over IGP was observed to be 4 times greater than the EIO region during the transition phase (figure 13a), 3 times during the advancing period (figure 13b), and 2 times during the peak period (figure 13c). The atmospheric aerosol radiative forcing over the IGP and EIO shows a dipole pattern, this can cause an increase in surge of pre-monsoon westerlies. Over the IGP, the atmospheric radiative forcing varies between. The difference in ARF in the atmosphere between IGB and EIO was noticed to be very high during the initial phase of the monsoon (transition phase) and gradually decreased towards the peak phase of the monsoon.

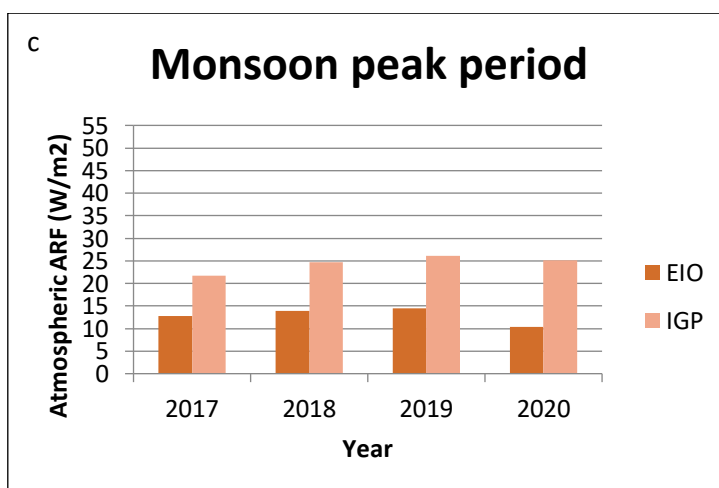
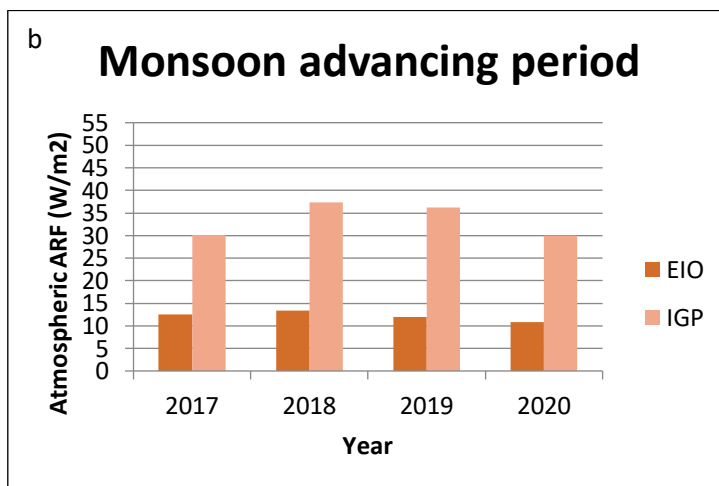
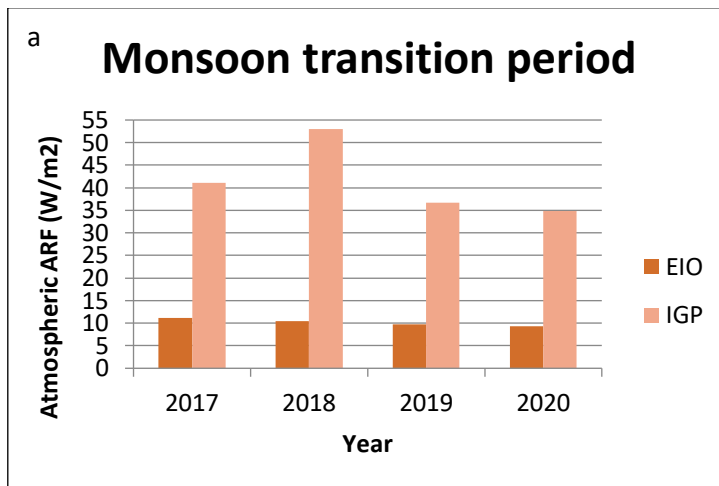
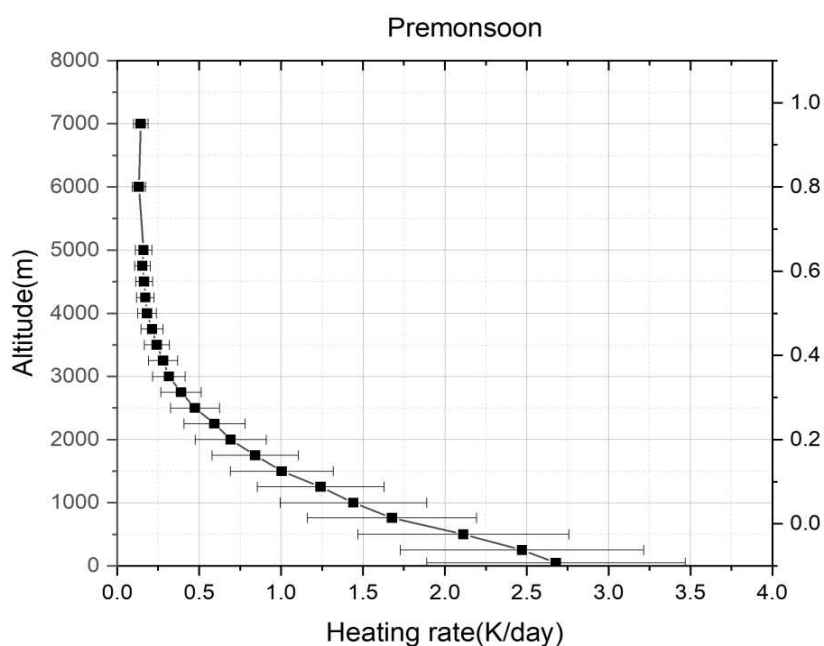


Figure 13: Graphical representation of aerosol induced atmospheric radiative forcing over Indo Gangetic Plain and Equatorial Indian Ocean during a) transition phase, b) advancing phase, and c) peak phase.

#### 4.6. ATMOSPHERIC HEATING RATE

The absorption and scattering of solar radiation by aerosols and associated radiation interactions modulates the vertical temperature profile of the atmosphere, which has an impact on atmospheric stability. The atmospheric heating rate in the IGB region has been observed to be quite high during the pre-monsoon period compared to monsoon and post-monsoon period as shown by the figure 14. The heating rate is generally higher in the lower atmosphere and drops exponentially with height. The averaged maximum value of aerosol induced heating rate was found at the surface was  $2.68 \pm K/day$  during pre-monsoon period and further reduced during monsoon ( $1.48 \pm 0.56 K/day$ ) and post monsoon periods ( $1.17 \pm 0.44$ ). According to the heating rate profile across the IGP, increased aerosol loading and associated strong radiative forcing impart maximum amplitude of heating rate near the surface and become minimum at the upper troposphere levels.





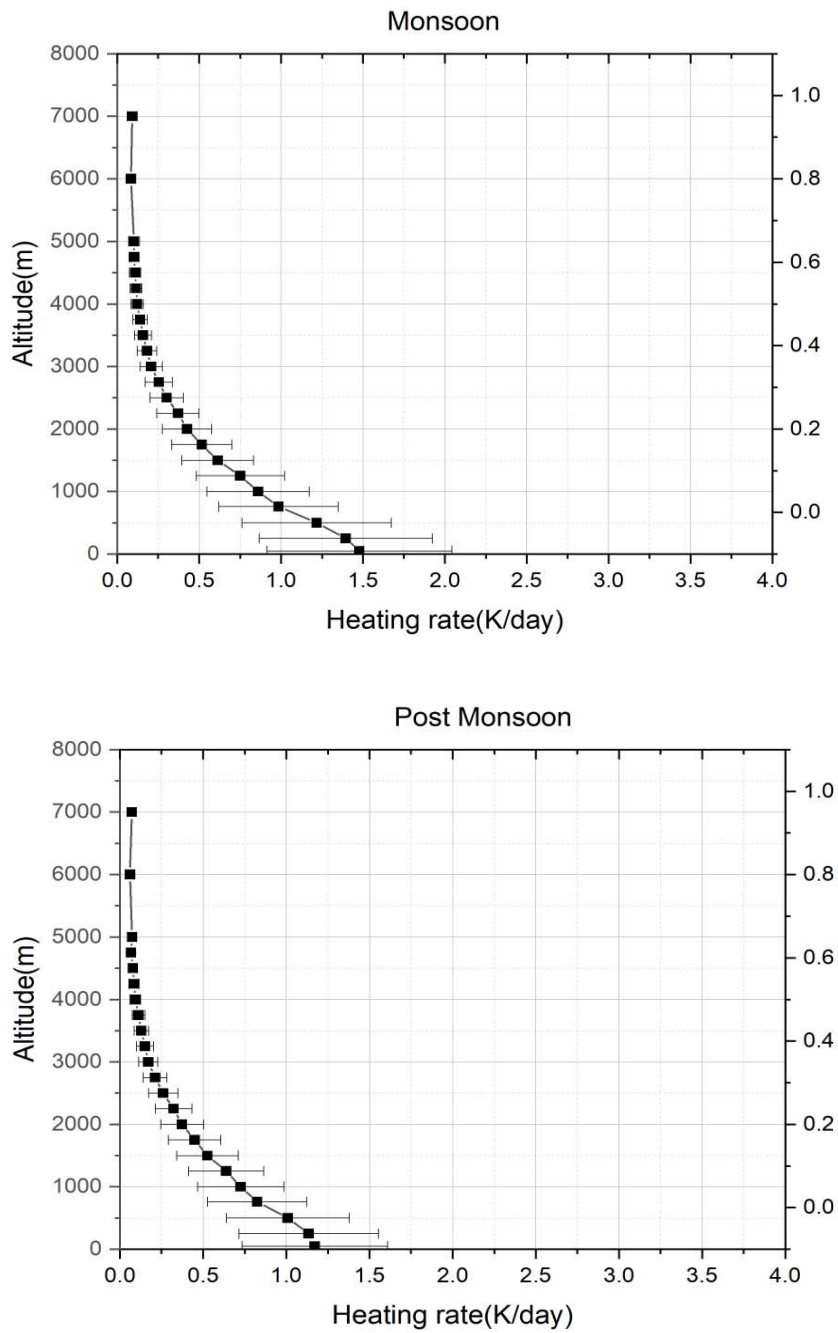


Figure 14: Vertical profile for aerosol induced heating rate over the Indo Gangetic Plain during pre-monsoon, monsoon and post-monsoon.

#### 4.7. AEROSOL-PRECIPIATION CORRELATION

The study investigates the possible connection between aerosol burden and precipitation over Kerala and IGP region to examine regional sensitivity of

aerosols. To interpret the relationship between aerosol loading and precipitation rate we used CERES daily mean AOD datasets @ 550nm as a function of aerosol loading and high resolution gridded daily rainfall dataset prepared by the IMD was utilized for surface rainfall data. We analyze AOD and precipitation over the IGB region and Kerala for 21 days during 2017 – 2020, in which 10 days before and after the date of MOK were considered.

Over Kerala, for every year from 2017 – 2020 Light rain spells were noted during the 1<sup>st</sup> phase (10 days before MOK) and moderate rainfall was received during the 2<sup>nd</sup> phase (figure 15a). Daily mean value of AOD during the first phase remains quite good with a varying range of 0.5 to 0.8. During the second phase the rate of aerosol concentration showed a sharp decline with a range of 0.3 to 0.5 due to wash out effect. The rate of precipitation during the second phase shoot up at a rate of 2 to 3, while the rate aerosol loading downturn by two times. Averaged over the individual spells a sharp rise in AOD during the advancement of the second phase was observed except in the year 2019. The year 2019 noticed a slight fall in daily average AOD during the second phase (0.68) relative to the former phase (0.74), concurrently a rise in light rain spells were also observed during the same period. Individual very light and light rainfall spells whose intensity and duration are variable, the amount of average daily rainfall were found to be between 2 to 6mm.

Average AOD values lie between 0.65 and 0.98 suggest a relatively higher concentration of aerosols in the IGB region indicating a possible influx of westerly wind-driven dust from adjacent desert regions of Arabia, Africa, and Thar (figure 15b). It is clear that the value of AOD drops to a minimum shortly after excessive rainfall. Throughout the study period, total aerosol loading is found to be significantly higher over the IGB region than in Kerala. The examination of AOD and rainfall over Kerala revealed that AOD anomalies have a nearly inverse relationship with rainfall, which can be attributed to wet scavenging and a lack of emission sources. The onset of monsoon, which is accompanied by a rapid increase in precipitation levels, plays a significant role in

limiting aerosol concentration over Kerala. During the advancing days of the studied period, a positive gradient of aerosol loading and rainfall was observed. Despite the fact that premonsoon thunderstorms were effective at removing particulate matter from the atmosphere through wet scavenging during the study period, a significant amount of aerosol concentration was found over the Indo Gangetic plain, indicating that there is the possibility of a constant source of aerosols and the region can be considered a reservoir of aerosols (figure 15c).

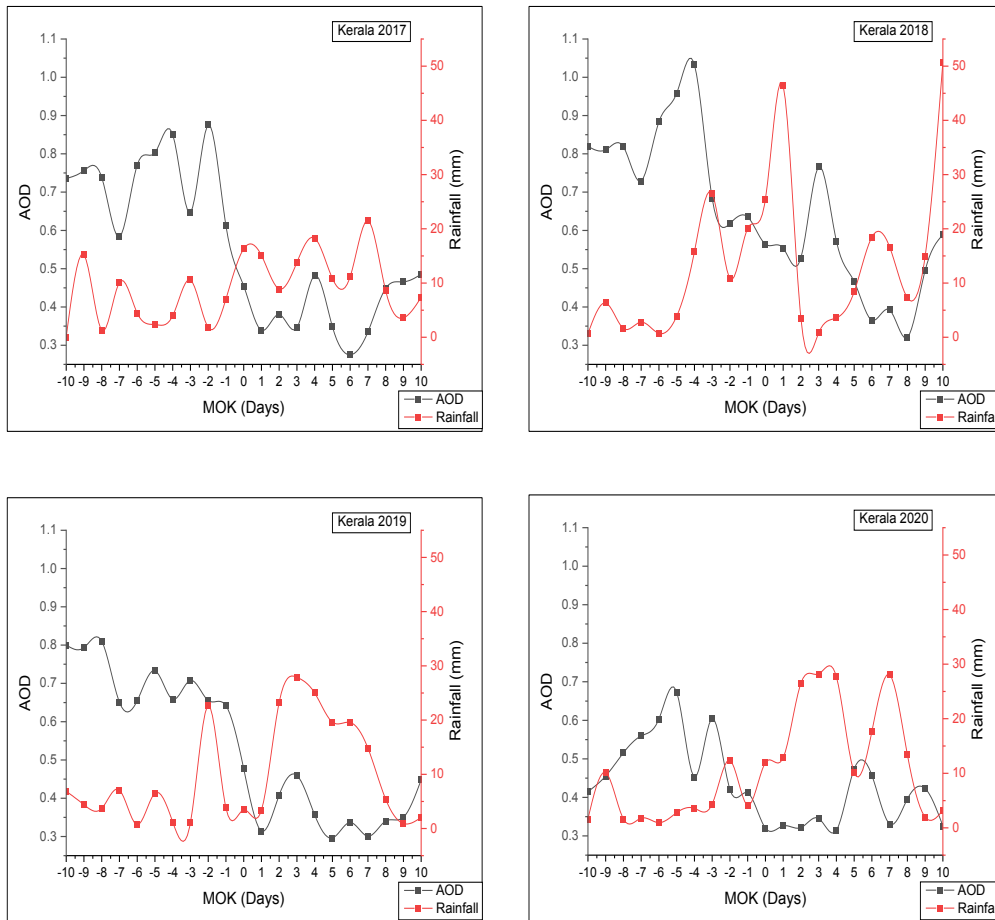


Figure 15a: AOD - rainfall association over Kerala showing 10 days before and after MOK over a period of 2017-2020

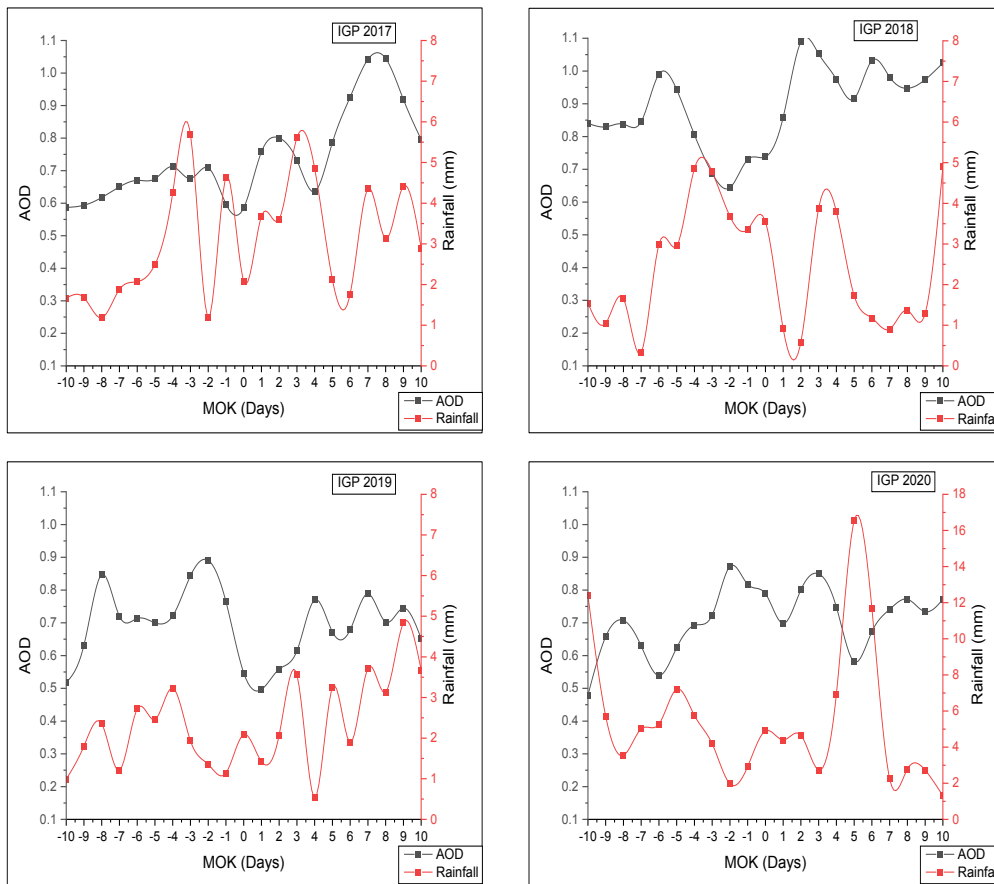


Figure 16b: AOD - rainfall association over IGP showing 10 days before and after MOK over a period of 2017-2020

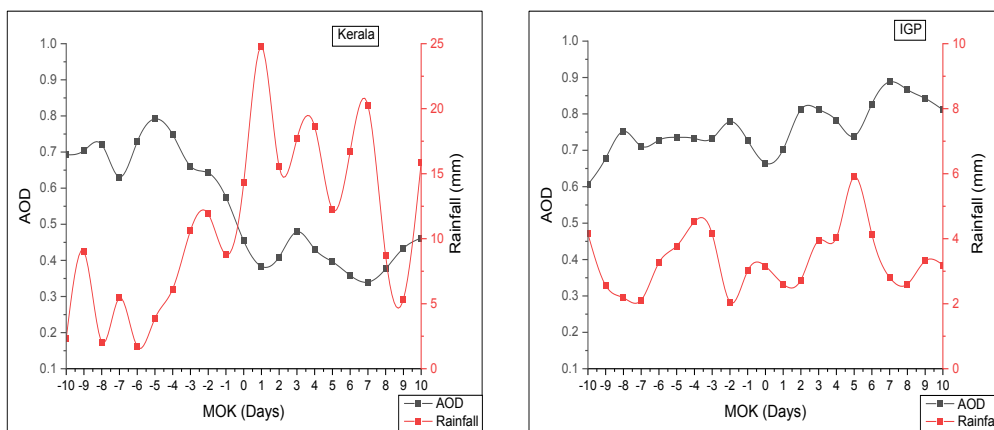


Figure 17c: Temporal average of AOD - rainfall over Kerala and IGP over a period of 2017-2020

## CHAPTER 5

### DISCUSSION

Aerosol mechanisms should be depicted in all dimensions in models to increase the realism of the simulated forcing component and to improve the predictability of future climate change. Aerosols impact the earth energy budget in a variety of ways depending on the nature of the emission source, location, and vertical distribution, through direct, indirect, semi direct, and associated thermodynamic changes. In this regard, a multiplatform based approach is required to analyse the integrated response of aerosols. We investigated seasonal and intraseasonal variations in the spatial and temporal distribution of aerosols during the summer monsoon using aerosol optical depth (AOD) daily data has been taken from the MODIS instrument onboard the Terra platform. According to the findings, aerosols were abundant during the summer monsoon, with regional variation in their spatial distribution. This could be attributed to changes in emission sources, topography, and ambient climate conditions. In this study, we focused on aerosol forcing during the transition phase, so we needed to look at aerosol concentration during this sub-phase as well as compare it to other monsoon sub-phases. We discovered that during the sub-phases of the wet monsoon, aerosols showed a wide range of variability in their type and spatial distribution, which can have a significant impact on the regional climate system and associated large-scale circulation over the entire monsoon regime. Furthermore, their short lifespan adds to their complexity. Dust is the most common type of aerosol over the study area, based on the current analysis of aerosol species contribution and then comes the sulphate and sea salt. So that mineral dust during the wet monsoon can be identified as a seasonal source. Within the season, the percentage distribution varies, and the spatial extent varies as well.

The reversal of westerlies from north to south during the transition phase of the summer monsoon plays a major role in controlling aerosol transport and distribution over the study area, as evidenced by the analysis of wind at 850hpa.

In the study aerosol index (AI) is used to determine the spatial distribution of absorbing aerosols during monsoon sub-phases. We found a similar pattern of spatial extent of aerosols over northern India and the northern Arabian Sea by comparing the spatial plots of AOD and AI implying that absorbing aerosols, primarily dust, play a major role over these regions during the wet monsoon. As a result, it is clear that taking a global average of aerosols and analysing their forcing effects will never provide precise information on aerosol radiative forcing because its concentration and distribution change within the local environment, necessitating regional-based analysis. Therefore, in addition to determining the aerosol radiative forcing in the atmosphere over the entire study area during the sub-phases of the wet monsoon, we chose two regions to measure regional aerosol-induced radiative forcing in the atmosphere: one with a high aerosol load, IGP ( $75^{\circ}$ - $92^{\circ}$ E,  $22^{\circ}$ - $22^{\circ}$ N) and the other with a lower aerosol concentration, EIO ( $50^{\circ}$ - $95^{\circ}$ E,  $5^{\circ}$ S- $7^{\circ}$ N). We spotted an intriguing observation that, for all of the study years 2017-2020, the spatial average aerosol forcing over the entire monsoon season is approximately double that of EIO and roughly half that of IGP that again emphasising the importance of regional-based analysis. Over both the IGP and the EIO, the net radiative forcing of aerosols in the atmosphere, as well as over the TOA, results in an overall warming, while over the surface, a dimming effect occurs (cooling effect). The warming caused by aerosols in the atmosphere is 3-4 times greater than at the TOA. It was also observed that during the transition phase, atmospheric aerosol radiative forcing over the IGP is 4 times higher than that over the EIO, but as the monsoon progressed, this difference decreased, indicating a reduction in aerosol loading over the IGP in the subsequent phases. The radiative forcing is found to be greater in the northern part of the Indian monsoon region than in the southern part, which is attributed to higher aerosol loading in the northern part as a result of dust events during the summer monsoon. Therefore, much effort is required to study the aerosol parameters and variability in northern India, particularly in the Indo-Gangetic basin region, which is one of the world's most densely populated basins.

In the study we also determine atmospheric heating rate over the IGP during pre-monsoon, monsoon, and post-monsoon periods was also identified as a region characterised by significant aerosol loading and associated high aerosol radiative forcing. It was revealed that the heating rate is higher at lower altitudes and gradually decreases with altitude, indicating a higher aerosol impact in the lower atmosphere than in the upper atmosphere; additionally, the heating rate is higher during the pre-monsoon period and reduces as the monsoon progresses over the region. We chose two regions over the Indian subcontinent, the IGP and Kerala, to study the regional impact of precipitation on aerosol loading during the Indian monsoon. During the investigation, we observed a sharp decrease in aerosol loading over Kerala shortly after the monsoon began, whereas the trend was insignificant over the IGP. However, it is clear that the aerosol concentration decreased with each individual spike in precipitation, indicating that aerosols have a short residence period due to the impact of wet deposition in and below clouds, as well as the washout effect caused by precipitation. It's possible that the lack of a significant trend over the IGP region is due to the presence of constant aerosol emission sources. The aerosol radiative forcing and associated heating rate are higher during the transition phase of the monsoon compared to the other sub-phases, indicating the importance of these phases in controlling monsoon circulation, which accounts for approximately 80% of monsoon rainfall in India. Aerosols' radiative properties have a significant impact on the climate system, which controls the cooling/heating effect on the earth's surface and, as a result, the warming/cooling of the atmosphere. According to the findings of this study, we found that there is a two-way interaction between aerosol loading and large-scale monsoon circulation, with aerosol loading influencing monsoon circulation due to their specific radiative behaviour in controlling climate systems, and monsoon circulation influencing aerosol transport and loading due to changes in precipitation and wind pattern.

## CHAPTER 6

### SUMMARY

There exist a complex nature of interaction between aerosol and radiation. The interactions between aerosols and radiation, as well as its regional and global consequences, are one of the least known and most uncertain aspects of climate research. The anomalous westerly low level wind from dry to semi-arid regions such as Africa, west Asia, and the Thar Desert can transport aerosols, particularly mineral dust, resulting in dust loading over the Indo-Gangetic plain and north-western India. The Indian monsoon region has been found as having a high concentration of atmospheric aerosols and, by their radiative forcing, have a considerable impact on the summer monsoon hydrological cycle. The investigation of AOD and rainfall over Kerala indicated that AOD anomalies had a roughly inverse relationship with rainfall, which can be attributed to wet scavenging and a lack of emission sources. The key conclusions are:

- The IGP is a region with a unique topography that is regarded to be one of the world's most polluted and highly populated areas. These unique characteristics keep a heavy burden of aerosols over the IGP and also exhibit substantial inter-seasonal and intra-seasonal variations. A strong gradient in aerosol concentrations over the IGP has a significant impact on the energy budget.
- The aerosol radiative forcing are found to be higher in the northern part of the Indian monsoon regime, particularly in the IGP region, than in the southern part, which can be due to higher aerosol loading in the northern part, which can be attributed to long-distance transport of aerosols from western arid regions, increasing population, urbanisation, and industrialization.
- There exist a dipole pattern in radiative forcing between IGP and EIO, which can induce southward shift of monsoon front.
- Thar-Pakistan deserts, Arabian deserts, and Taklimakan deserts identified as important key source sites for the high loading of absorbing aerosols around the research area.



- Our findings are line with the observations of Lau and Kim (2006), who found that absorbing aerosol emission, concentration, and transport are affected by large-scale circulation and rainfall, and that total dust loading in all three key source regions (Thar-Pakistan deserts, Arabian deserts, and Taklimakan deserts) is subject to multi-scale variability associated with the monsoon climate system.
- During the pre-monsoon period, an enhanced aerosol induced heating rate is observed over the northern regions of the Indian subcontinent compared to the remaining monsoon periods, which can be related to the accumulation of absorbing aerosol combined with local aerosol emission.
- Our evaluation reveals a clear negative aerosol-rainfall association across Kerala, because an immediate decline in aerosol concentration occurs after the arrival of monsoon, which may be attributed to the likely effect of wet scavenging. Whereas an insignificant correlation was detected over the IGP, this can be attributed to the region's consistent source of aerosols. Quick deposition of absorbing aerosols across the IGP region following each rainfall event indicates a high aerosol emission rate and geography-induced accumulation.
- Aerosols physical properties are also strongly influenced by their origins, which are widely dispersed and vary greatly from one place to another. As a result, the aerosol impact on the climate system has a strong regional component, and changes in regional aerosol loading not only affect the radiation balance directly but also indirectly affect cloud characteristics, causing the hydrological cycle to be disrupted.
- Estimating aerosol radiative forcing values at the surface, TOA, and atmosphere on a global scale can be highly uncertain due to uncertainties in the geographical distribution of aerosols, emission sources, optical characteristics, terrain, and meteorological parameters. As a result, there is a need to acquire information on radiative forcing at the local scale in various climatic zones to reduce uncertainties.
- The findings show that aerosols could be a potential mediator in interannual precipitation modulation during the southwest monsoon.

## CHAPTER 7

### REFERENCES

- Ahmad, S. P., Torres, O., Bhartia, P. K., Leptoukh, G. and Kempler, S. (2006). *Aerosol index from TOMS and OMI measurements. 86th AMS Annual Meeting. 86th AMS Annual Meeting.*
- Albrecht, B. A. 1989. Aerosols, Cloud Microphysics, and Fractional Cloudiness. *Science. 245(4923): pp.1227-1230.*
- Al-Salihi, A. M. 2018. Characterization of aerosol type based on aerosol optical properties over Baghdad, Iraq. *Arab.J.Geosci. 11.* doi:<https://doi.org/10.1007/s12517-018-3944-1>
- AL-Taie, K. B., Rajab, J. M. and Al-Salihi, A. M. 2020. Climatology and classification of aerosols based on optical properties over selected stations in Iraq. 2090. AIP Conference Proceedings. doi:<https://doi.org/10.1063/5.0031471>
- Andronache, C., Donner, L. J., Seman, C. J. and Hemler, R. S. 2002. A study of the impact of the Intertropical Convergence Zone on aerosols during INDOEX. *J. Geophys. Res., 107(D19): pp.26-16.* doi:<https://doi.org/10.1029/2001JD900248>
- Ansmann, A. and Müller, D. 2005. Lidar and Atmospheric Aerosol Particles. In *Lidar. Springer Series in Optical Sciences* (Vol. 102, pp. 105-141). Springer, New York, NY. doi:[https://doi.org/10.1007/0-387-25101-4\\_4](https://doi.org/10.1007/0-387-25101-4_4)
- Arya, V. B., Sajani, S. and Kavirajan, R. 2021. On the build-up of dust aerosols and possible indirect effect during Indian summer monsoon break spells using recent satellite observations of aerosols and cloud properties. *J. Earth Syst. Sci., 130(1).*doi:[https://ui.adsabs.harvard.edu/link\\_gateway/2021JESS..130...42A/doi:10.1007/s12040-020-01526-6](https://ui.adsabs.harvard.edu/link_gateway/2021JESS..130...42A/doi:10.1007/s12040-020-01526-6)

- Babu, S. S., Manoj, M. R., Moorthy, K. K., Gogoi, M. M., Nair, V. S., Kompalli, S. K., Satheesh, S. K., Niranjana, K., Ramagopal, K., Bhuyan, P. K. and Singh, D. 2013. Trends in aerosol optical depth over Indian region: Potential causes and impact indicators. *J. Geophys. Res. Atmos.*, *118*(20), 11,794-11,806. doi:<https://doi.org/10.1002/2013JD020507>
- Bibi, H., Alam, K. and Bibi, S. 2017. Estimation of shortwave direct aerosol radiative forcing at four locations on the Indo-Gangetic plains: Model results and ground measurement. *Atmos. Environ.*, *163*: pp.166-181. doi:<https://doi.org/10.1016/J.ATMOSENV.2017.05.043>
- Bollasina, M. A., Ming, Y. and Ramaswamy, V. 2011. Anthropogenic Aerosols and the Weakening of the South Asian Summer Monsoon. *science*, *334*(6055): pp.502-505. doi:10.1126/science.1204994
- Bollasina, M. A., Ming, Y., and Ramaswamy, V. 2013. Earlier onset of the Indian monsoon in the late twentieth century: The role of anthropogenic aerosols. *Geophys. Res. Lett.*, *40*(14): pp.3715-3720. doi:<https://doi.org/10.1002/grl.50719>
- Bollasina, M., Nigam, S., and Lau, K.-M. 2008. Absorbing Aerosols and Summer Monsoon Evolution over South Asia: An Observational Portrayal. *J. Clim.*, *21*(13): pp.3221–3239. doi:<https://doi.org/10.1175/2007JCLI2094.1>
- Boucher, O. 2015. Atmospheric Aerosols. *In: Atmospheric Aerosols*: pp. 9-14. Springer, Dordrecht. doi:[https://doi.org/10.1007/978-94-017-9649-1\\_2](https://doi.org/10.1007/978-94-017-9649-1_2)
- Buchard, V., Silva, A. M., Colarco, P. R., Darmenov, A., Randles, C. A., Govindaraju, R., Torres, O., Campbell, J., and Spurr, R. 2015. Using the OMI aerosol index and absorption aerosol optical depth to evaluate the NASA MERRA Aerosol Reanalysis. *Atmos. Chem. Phys.*, *15*(10): pp.5743-5760. doi:<https://doi.org/10.5194/acp-15-5743-2015>
- Choudhury, G., Tyagi, B., Vissa, N. K., Singh, J., Sarangi, C., Tripathi, S. N., and Tesche, M. 2020. Aerosol-enhanced high precipitation events near the

- Himalayan foothills. *Atmos. Chem. Phys.*, 20(23): pp.15389–15399. doi:<https://doi.org/10.5194/acp-20-15389-2020>
- Chung, C. E., and Ramanathan, V. 2006. Weakening of North Indian SST Gradients and the Monsoon Rainfall in India. *J. Clim.*, 19(10): pp.2036–2045. doi:<https://doi.org/10.1175/JCLI3820.1>
- Collier, J. C., and Zhang, G. J. 2009. Aerosol direct forcing of the summer Indian monsoon as simulated by the NCAR CAM3. *Clim Dyn*, 32: pp.313-332. doi: <https://doi.org/10.1007/s00382-008-0464-9>
- Contini, D., Vecchi, R., and Viana, M. 2018. Carbonaceous Aerosols in the Atmosphere. *Atmosphere*, 9(5). doi:<https://doi.org/10.3390/atmos9050181>
- Dave, P., Bhushan, M., and Venkataraman, C. 2017. Aerosols cause intraseasonal short-term suppression of Indian monsoon rainfall. *Sci Rep* 7. doi: <https://doi.org/10.1038/s41598-017-17599-1>
- Ekman, A. M. 2012. Aerosol particles and their seasonal variability: Are aerosol particles important for seasonal prediction? *ECMWF Annual Seminar*, (pp. 195-206). doi:<https://www.ecmwf.int/node/14836>
- Gautam, R., Hsu, N. C., Lau, K.-M., and Kafatos, M. 2009. Aerosol and rainfall variability over the Indian monsoon region: distributions, trends and coupling. *Ann. Geophys.* 27(9): pp.3691–3703. doi:<https://doi.org/10.5194/angeo-27-3691-2009>
- Gautam, R., Hsu, N. C., Tsay, S. C., Lau, K. M., Holben, B., Bell, S., Smirnov, A., Hansell, R., Ji, Q., Parya, S., Aryal, D., Kayastha, R. and Kim, K. M. 2011. Accumulation of aerosols over the Indo-Gangetic plains and southern slopes of the Himalayas: distribution, properties and radiative effects during the 2009 pre-monsoon Season. *Atmos. Chem. Phys.* 11(24): pp.12841–12863. doi:<https://doi.org/10.5194/acp-11-12841-2011>
- Grandey, B. S., Rothenberg, D., Avramov, A., Jin, Q., Lee, H.-H., Liu, X., Lu, Z., Samuel, A. and Wang, C. 2018. Effective radiative forcing in the aerosol–

- climate model CAM5.3-MARC-ARG. *Atmos. Chem. Phys.* 18(21):pp. 15783–15810. doi:<https://doi.org/10.5194/acp-18-15783-2018>
- Guleria, R. P. and Kuniyal, J. C. 2016. Characteristics of atmospheric aerosol particles and their role in aerosol radiative forcing over the northwestern Indian Himalaya in particular and over India in general. *Air Qual Atmos Health*(9): pp.795–808. doi:<https://doi.org/10.1007/s11869-015-0381-0>
- Hansen, J., Sato, M., and Ruedy, R. 1997. Radiative forcing and climate response. *J. Geophys. Res.*, 102(D6): pp.6831-6864. doi:10.1029/96JD03436
- Harshvardhan. 1993. Chapter 3 Aerosol-Climate Interactions. In P. V. Hobbs (Ed.), *Aerosol–Cloud–Climate Interactions* (Vol. 54, pp.75-95). Academic Press. doi:[https://doi.org/10.1016/S0074-6142\(08\)60212-0](https://doi.org/10.1016/S0074-6142(08)60212-0)
- Haywood, J., and Boucher, O. 2000. Estimates of the direct and indirect radiative forcing due to tropospheric aerosols: A review. *Rev. Geophys.*, 38(4): pp. 513-543. doi:<https://doi.org/10.1029/1999RG000078>
- Holben, B. N., Tanré, D., Smirnov, A., Eck, T. F., Slutsker, I., Abuhassan, N., Newcomb, W. W., Schafer, J. S., Chatenet, B., Lavenu, F., Kaufman, Y. J., Vande Castle, J., Setzer, A., Markham, B., Clark, D., Frouin, R., Halthore, R., Karneli, A., O'Neill, N. T., Pietras, C., Pinker, R. T., Voss, K. and Zib, G. 2001. An emerging ground-based aerosol climatology: Aerosol optical depth from AERONET. *J. Geophys. Res.*, 106(D11): pp.12067-12097. doi:<https://doi.org/10.1029/2001JD900014>
- Huang, J., Wang, T., Wang, W., Li, Z., & Yan, H. (2014). Climate effects of dust aerosols over East Asian arid and semiarid regions. *J. Geophys. Res. Atmos.*, 119(19), p.11,398-11,416.
- IPCC (Intergovernmental Panel on Climate Change) 2001. Aerosols, their Direct and Indirect Effects. *Climate Change: The Scientific Basis*, pp.289-348.
- IPCC (Intergovernmental Panel on Climate Change) 2007. Climate Change 2007: Summary for Policymakers. In: Parry, M.L., Canziani, O.F., Palutikof, J.P., van der Linden, P.J. and Hanson, C.E. (Eds.). *Climate Change 2007:*

Impacts, Adaptation and Vulnerability. Contribution of Working Group II to the Fourth Assessment Report of the Intergovernmental Panel on Climate Change.

- Jaenicke, R. (1993). Tropospheric Aerosols. In P. V. Hobbs (Ed.), *International Geophysics* (Vol. 54, pp. 1-31). doi:[https://doi.org/10.1016/S0074-6142\(08\)60210-7](https://doi.org/10.1016/S0074-6142(08)60210-7)
- Johnson, B. T., Shine, K. P., and Forster, P. M. 2003. The semi-direct aerosol effect: Impact of absorbing aerosols. *Q. J. R. Meteorol. Soc.*, 130(599): pp. 1407–1422. doi: 10.1256/qj.03.61
- Kant, Y., Singh, A., Mitra, D., Singh, D., Srikanth, P., Madhusudanacharyulu, A. S., and Murthy, Y. N. 2015. Optical and Radiative Properties of Aerosols over Two Locations in the North-West Part of India during Premonsoon Season. *Adv. Meteorol.* doi:<https://doi.org/10.1155/2015/517434>
- Kaskaoutis, D. G., Sifakis, N., Retalis, A., and Kambezidis, H. D. 2010. Aerosol Monitoring over Athens Using Satellite and Ground-Based Measurements. *Adv. Meteorol.* pp.1-12. doi:<https://doi.org/10.1155/2010/147910>
- Kaufman, Y. J., Tanré, D., and Boucher, O. 2002. A satellite view of aerosols in the climate system. *Nature* , 419: pp.215-223. doi:<https://doi.org/10.1038/nature01091>
- Kedia, S., Ramachandran, S., Holben, B. N., and Tripathid, S. N. 2014. Quantification of aerosol type, and sources of aerosols over the Indo-Gangetic Plain. *Atmos. Environ.*, 98: pp.607-619. doi:<https://doi.org/10.1016/j.atmosenv.2014.09.022>.
- Kumar, M., Parmar, K., Kumar, D., Mhawish, A., Broday, D., Mall, R., and T.Banerjee. 2018. Long-term aerosol climatology over Indo-Gangetic Plain: Trend, prediction and potential source fields. *Atmos. Environ.*, 180: pp.37-50. doi:<http://dx.doi.org/10.1016/j.atmosenv.2018.02.027>
- Kumar, V. A., Pandithurai, G., Leena, P. P., Dani, K. K., Murugavel, P., Sonbawne, S. M., Patil, D. R. and Maheskumar, R. S. 2016. Investigation

- of aerosol indirect effects on monsoon clouds using ground-based measurements over a high-altitude site in Western Ghats. *Atmos. Chem. Phys.*, 16(13): pp.8423–8430. doi:<https://doi.org/10.5194/acp-16-8423-2016>
- Kumari, B. P., and Goswami, B. N. 2010. Seminal role of clouds on solar dimming over the Indian monsoon region. *Geophys. Res. Lett.*, 37(6), L06703.
- Lau, K., & Kim, K. 2006. Observational relationships between aerosol and Asian monsoon rainfall, and circulation. *Geophys. Res. Lett.*, 33(21). doi:<https://doi.org/10.1029/2006GL027546>
- Lau, K.-M., Ramanathan, V., Wu, G.-X., Li, Z., Tsay, S. C., Hsu, C., Sikka, R., Holben, B., Lu, D., Tartari, G., Chin, M., Koudelova, P., Chen, H., Ma, Y., Huang, J., Taniguchi, K. and Zhang, R. 2008. The Joint Aerosol–Monsoon Experiment: A New Challenge for Monsoon Climate Research. *Bulletin of the American Meteorological Society*, 86(3): pp.369–384.
- Lau, W. K. 2016. The Aerosol-Monsoon Climate System of Asia: A New Paradigm. *J.Meteorol.Res.*, 30(1): pp.1-11. doi:<https://doi.org/10.1007/s13351-015-5999-1>
- Lau, W. K., Kim, K.-M., Shi, J.-J., Matsui, T., Chin, M., Tan, Q., Peters-Lidard, C. and Tao, W. K. 2017. Impacts of aerosol–monsoon interaction on rainfall and circulation over Northern India and the Himalaya Foothills. *Clim. Dyn.*, 49: pp.1945-1960. doi:<https://doi.org/10.1007/s00382-016-3430-y>
- Lohmann, U., and Feichter, J. 2001. Can the direct and semi-direct aerosol effect compete. *Geophys. Res. Lett.*, 28(1): pp.159-161. doi:<https://doi.org/10.1029/2000GL012051>
- Manoj, M. G., Devara, P. C., Safai, P. D., and Goswami, B. N. 2011. Absorbing aerosols facilitate transition of Indian monsoon break to active spells. *Clim.Dyn*, 37: pp.2181–2198.

- Manoj, M. G., Devara, P., Joseph, S., and Sahai, A. 2012. Aerosol indirect effect during the aberrant Indian Summer Monsoon breaks of 2009. *Atmos. Environ.*, 160: pp. 153-163.
- Martins, J. A., and Dias, M. A. 2009. The impact of smoke from forest fires on the spectral dispersion of cloud droplet size distributions in the Amazonian region. *Environ. Res. Lett.*, 4, 015002.
- Mehta, M. (2015). A study of aerosol optical depth variations over the Indian region using thirteen years (2001-2013) of MODIS and MISR Level 3 data. *109*: pp.161-170. doi:doi:10.1016/j.atmosenv.2015.03.021
- Mitchell, J. F., & Johns, T. C. (1997). On Modification of Global Warming by Sulfate Aerosols. *J. Climate*, 10(2): pp.254-267. doi:https://doi.org/10.1175/15200442(1997)010%3C0245:OMOGWB%3E2.0.CO;2
- Moorthy, K. K., Babu, S. S., Manoj, M. R., & Satheesh, S. K. (2013). Buildup of aerosols over the Indian Region. *Geophys. Res. Lett.*, 40(5): pp.1011-1014.
- Nair, V. S., Babu, S. S., Manoj, M. R., Moorthy, K. K., & Chin, M. (2017). Direct radiative effects of aerosols over South Asia from observations and modeling. *Clim.Dyn*, 49: pp.1411–1428. doi:https://doi.org/10.1007/s00382-016-3384-0
- Onyeuwaoma, N. D., Chineke, T. C., Nwofor, O. K., Crandell, I., Awe, O. O., Olasumbo, A., Opara, A. I., Pius, N., Tochukwu, M, Joy, N. and Hassan, M. M. 2018. Characterization of aerosol loading in urban and suburban locations: Impact on atmospheric extinction. *Cogent Environ. Sci.*, 4(1). doi:https://doi.org/10.1080/23311843.2018.1480333
- Pandey, S. K., Vinoj, V., Landu, K., and Babu, S. S. 2017. Declining pre-monsoon dust loading over South Asia: Signature of a changing regional climate. *Sci.Rep.*, 7(1). doi:https://doi.org/10.1038/s41598-017-16338-w



- Pandithurai, G., Pinker, R. T., Takamura, T., and Devara, P. C. 2004. Aerosol radiative forcing over a tropical urban site in India. *Geophys. Res. Lett.*, *31*(12). doi:<https://doi.org/10.1029/2004GL019702>
- Panicker, A., Pandithurai, G., and Dipu, S. 2010. Aerosol indirect effect during successive contrasting monsoon seasons. *Atmos. Environ.*, *44*(15): pp.1937-1943.
- Rajeev, K., and Ramanathan, V. 2002. The Indian ocean experiment: aerosol forcing obtained from satellite data. *Adv. Space Res.*, *29*(11): pp.1731-1740. doi:[https://doi.org/10.1016/S0273-1177\(02\)00086-8](https://doi.org/10.1016/S0273-1177(02)00086-8)
- Ramachandran, S., and Cherian, R. 2008. Regional and seasonal variations in aerosol optical characteristics and their frequency distributions over India during 2001–2005. *J. Geophys. Res.*, *113*(D18).
- Ramachandran, S., & Kedia, S. 2013. Aerosol-Precipitation Interactions over India: Review and Future Perspectives. (A. I. Calvo, Ed.) *Advances in Meteorology*, 2013: pp.1687-9309.
- Ramanathan, V., Crutzen, P. J., Kiehl, J. T. and Rosenfeld, D. 2001. Aerosols, Climate, and the Hydrological Cycle. *294*(5549): pp.2119-2124.
- Ramanathan, V., Crutzen, P. J., Lelieveld, J., Mitra, A. P., Althausen, D., Anderson, J., Andreae, M. O., Cantrell, W., Cass, G. R., Chung, C. E., Clarke, A. D., Coakley, J. A., Collins, W. D., Conant, W. C., Dulac, F., Heintzenberg, J., Heymsfield, A. J., Holben, B., Howell, S., Hudson, J., Jayaraman, A., Kiehl, J.T., Krishnamurti, T. N., Lubin, D., McFarquhar, G., Novakov, T., Ogren, J. A., Podgorny, I. A., Prather, K., Priestley, K., Prospero, J. M., Quinn, P. K., Rajeev, K., Rasch, P., Rupert, S., Sadourny, R., Satheesh, S. K. Shaw, G.E., Sheridan, P. and Valero, F. P. J. 2001. Indian Ocean Experiment: An integrated analysis of the climate forcing and effects of the great Indo-Asian haze. *J. Geophys. Res.*, *106*(D22): pp.28371-28398. doi:<http://dx.doi.org/10.1029/2001JD900133>

- Ridley, H. E., Asmerom, Y., Baldini, J. U., Breitenbach, S. F., Aquino, V. V., Pruffer, C., Culleton, B. J., Polyak, V., Lechleitner, F. A., Kennett, D. J., Zhang, M., Marwan, N., Macpherson, C. G., Baldini, L. M., Xiao, T., Peterkin, J. L., Awe, J. and Haug, G. H. 2015. Aerosol forcing of the position of the intertropical convergence zone since AD 1550. *Nature Geosci.*, 8: pp.195-200. doi:<https://doi.org/10.1038/ngeo2353>
- Rizza, U., Mancinelli, E., Morichetti, M., Passerini, G. and Virgili, S. 2019. Aerosol Optical Depth of the Main Aerosol Species over Italian Cities Based on the NASA/MERRA-2 Model Reanalysis. *Atmosphere*, 10(11). doi:<https://doi.org/10.3390/atmos10110709>
- Dipu, S., Prabha, V., Pandithurai, G., Dudhia, J., Pfister, G., Rajesh, K., and Goswami, B. N., 2013. Impact of elevated aerosol layer on the cloud macrophysical properties prior to monsoon onset. *Atmos. Environ.*, 70: pp. 454-467. doi:<https://doi.org/10.1016/j.atmosenv.2012.12.036>
- Tiwaria, S., Srivastava, A. K. and Singh, A. K., 2013. Heterogeneity in pre-monsoon aerosol characteristics over the Indo-Gangetic Basin. *Atmos. Environ.*, 77: pp.738-747.
- Saha, A., Moorthy, K. K. and Niranjana, K. 2005. Interannual Variations of Aerosol Optical Depth over Coastal India: Relation to Synoptic Meteorology. *J. Appl. Meteorol. Climatol.*, 44(7): pp.1066–1077. doi:<https://doi.org/10.1175/JAM2256.1>
- Sajani, S., Moorthy, K. K., Rajendran, K. and Nanjundiah, R. S. 2012. Monsoon sensitivity to aerosol direct radiative forcing in the community atmosphere model. *J Earth Syst Sci*, 121, 867–889. doi:<https://doi.org/10.1007/s12040-012-0198-2>
- Sarangi, C., Tripathi, S. N., Kanawade, V. P., Koren, I. and Pai, D. S. 2017. Investigation of the aerosol–cloud–rainfall association over the Indian summer monsoon region. *Atmos. Chem. Phys.*, 17(8):pp.5185-5204. doi:<https://doi.org/10.5194/acp-17-5185-2017>

- Sarkar, S., Chokngamwong, R., Cervone, G., Singh, R. P. and Kafatos, M. (2006). Variability of aerosol optical depth and aerosol forcing over India. *Adv. Space Res.*, 37(12): pp.2153-2159. doi:<https://doi.org/10.1016/j.asr.2005.09.043>
- Shaeb, K. H. 2019. Aerosol Studies over Central India. In M. Ince, and O. K. Ince (Eds.), *Hydrocarbon Pollution and its Effect on the Environment* (pp. 31-51). doi:10.5772/intechopen.85001
- Sivan, C. and Manoj, M. G. 2019. Aerosol and cloud radiative forcing over various hot spot regions. *Adv. Space Res.*, 64(8): pp.1577–1591.
- Sivaprasad, P., and Babu, C. A. 2016. Distribution and transport of aerosols in the south Indian region and surroundings. *Int. J. Remote Sens.*, 37(20). doi:<https://doi.org/10.1080/01431161.2016.1225174>
- Srivastava, A. K., Dey, S., & Tripathi, S. N. 2012. *Aerosol Characteristics over the Indo-Gangetic Basin: Implications to Regional Climate* (Vol. 3).
- Subba, T., Gogoi, M. M., Pathak, B., Bhuyan, P. K. and Babu, S. S. 2020. Recent trend in the global distribution of aerosol direct radiative forcing from satellite measurements. *Atmos Sci Lett.*, 21(11), e975.
- Torres, O., Bhartia, P. K., Herman, J. R., Ahmad, Z. and Gleason, J. 1998. Derivation of aerosol properties from satellite measurements of backscattered ultraviolet radiation: Theoretical basis. *J. Geophys. Res. Atmos.*, 103(D14): pp.17099-17110.
- Verma, S., Prakash, D., Soni, M., & Ram, K. (2019). Atmospheric Aerosols Monitoring: Ground and Satellite-Based Instruments. In *Environmental Monitoring and Assessment* (pp. 67-80). Intechopen. doi:10.5772/intechopen.80489
- YanGe Zhang, J. X., Shi, J., Xie, C., Ge, X., Wang, J., Kang, S., & Zhang, Q. 2017. Light absorption by water-soluble organic carbon in atmospheric fine particles in the central Tibetan Plateau. *Environ Sci Pollut Res*, 24: pp. 21386–21397. doi: <https://doi.org/10.1007/s11356-017-9688-8>

## ABSTRACT

The study estimates (i) aerosol radiative forcing over the Indian monsoon region as well as atmospheric heating rates, (ii) the spatial distribution of aerosols across the study area, and the relative contributions of different aerosol species and (iii) the aerosol-rainfall association by focusing at the regional influence of aerosol loading on precipitation. During the transition, northward progression (advance), and peak phases of the monsoon, the seasonally averaged aerosol radiative forcing at the surface was found to be negative, whereas at the top of the atmosphere it was shown to be positive. Aerosol radiative effects differ significantly globally because regions are characterized by different types of aerosol sources and meteorological conditions; thus, for a comprehensive examination of aerosol and radiative properties on a regional scale, we chose two regions: the Indo Gangetic Plain (IGP), which has a high aerosol burden, and the Equatorial Indian Ocean (EIO), which has a low aerosol burden. The climatologically averaged atmospheric Heating Rate associated with atmospheric radiative forcing during pre-monsoon, monsoon, and post-monsoon seasons were computed using the data inferred from the SBDART model. During the transition phase of the monsoon season from 2001 to 2017, the estimated mean aerosol radiative forcing values over IGP at the surface, TOA, and atmosphere were  $-31.96 \text{ Wm}^{-2}$ ,  $9.45 \text{ Wm}^{-2}$ , and  $41.4 \text{ W/m}^2$ , respectively, whereas over EIO it was  $-6.85 \text{ W/m}^2$ ,  $-3.30 \text{ W/m}^2$ , and  $-10.25 \text{ W/m}^2$ . Desert regions with much higher aerosol indexes than 2, such as the Thar-Pakistan deserts, Arabian deserts, and Taklimakan deserts, have been identified as large absorbing aerosol repositories that play a key role in maintaining higher aerosol forcing over the study area during the transition phase. The presence of absorbing aerosols was noticed to positively amplify the north-south temperature gradient, which can significantly alter large-scale monsoon circulation during the transition phase.